

DYNAMIC RESERVOIR TANK MODELING WITH
COUPLED WELLBORE MODEL

BRANDON G. THOMAS



**Dynamic Reservoir Tank Modeling with
Coupled Wellbore Model**

by

Brandon G. Thomas

A thesis submitted to the School of Graduate Studies in fulfillment of the thesis
requirement for the degree of Master of Engineering

Oil and Gas Engineering
Faculty of Engineering and Applied Science
Memorial University of Newfoundland

May 2012

St. John's, Newfoundland, Canada

Abstract

Modern reservoir engineering relies heavily on simulation models to provide a reliable prediction of the subsurface petroleum system. An ideal reservoir simulation model is one that represents the main features and behavior of a real system, but is simple enough to perform calculations in an efficient manner.

Using compressibility and transmissibility concepts, multiple reservoir tanks and flowing wellbores can be coupled to provide wellbore influx and inter-tank fluid transfer. This creates a series of ordinary differential equations that, when solved, can be used to describe the system's pressure and fluid movement pattern. This work uses these ordinary differential equations are efficiently solved using the Fourth-Order Runge-Kutta technique.

A flexible system of equations was created to represent 'n' number of communicating reservoir tanks which were then solved using ordinary differential equations for the first time.

This work demonstrates the successful integration of aquifers, reservoir tanks, well inflow, and wellbore modeling into an integrated system that can quickly be used as a tool for investigating petroleum systems. This work can form a fundamental module enabling the calculation of coupled wellbore and reservoir models with advanced completion technologies.

Acknowledgements

The author would like to acknowledge the generous and unwavering support of Heather, his loving wife.

A special acknowledgement is extended to Dr. Thormod E. Johansen, for providing supervision and direction to this body of work.

He would also like to acknowledge the financial support of his employer, Husky Energy Inc.

Table of Contents

| | |
|---|---------|
| Acknowledgements | iii |
| Table of Contents | iv |
| List of Figures | vii |
| List of Abbreviations, Nomenclature and Symbols | ix |
| List of Appendices | xii |
| 1.0 Introduction | - 13 - |
| 1.1 Scope of Research..... | - 16 - |
| 1.2 Thesis Outline..... | - 17 - |
| 1.3 Literature Review..... | - 18 - |
| 2.0 Background | - 22 - |
| 2.1 Reservoir Units..... | - 22 - |
| 2.2 Compressibility..... | - 22 - |
| 2.3 Transmissibility..... | - 25 - |
| 2.4 Aquifers..... | - 30 - |
| 2.5 Wellbore Flow Modeling..... | - 48 - |
| 3.0 Mathematical Development of Analytical Tank Modeling | - 61 - |
| 3.1 Exact Solution of Single Tank Modeling..... | - 62 - |
| 3.2 Single Tank with Aquifer..... | - 65 - |
| 3.3 Multiple Tanks with Multiple Aquifers..... | - 67 - |
| 3.4 Generalized Formulas..... | - 70 - |
| 3.5 Assumptions..... | - 73 - |
| 3.6 Other Scenarios..... | - 77 - |
| 3.7 Limits of Methodology Discussion..... | - 77 - |
| 3.8 Numerical Approach..... | - 79 - |
| 4.0 Results of Demonstration Cases | - 80 - |
| 4.1 Single Tank, No Aquifer..... | - 81 - |
| 4.2 Single Tank, With Aquifer..... | - 87 - |
| 4.3 Two Non-Communicating Tanks, With Common Aquifer..... | - 94 - |
| 4.4 Two Communicating Tanks, With Common Aquifer..... | - 101 - |
| 4.5 Three Non-Communicating Tanks, Without Aquifer..... | - 108 - |

| | | |
|-----------------|---|--------------|
| 4.6 | Three Partially-Communicating Tanks, With Partial Aquifer | 115 - |
| 4.7 | Comparison of Scenarios | 122 - |
| 5.0 | General Discussion of Results..... | 125 - |
| 5.1 | Novelty of Research..... | 126 - |
| 5.2 | Limitations | 126 - |
| 6.0 | Conclusions | 130 - |
| 7.0 | Recommendations | 132 - |
| Appendix | | 138 - |
| A. | Numerical Method Approach..... | 138 - |
| B. | Excel Main Calculation Sheet (Part A)..... | 142 - |
| C. | Flowing Wellbore and Reservoir Solver..... | 144 - |

List of Tables

| | |
|---|--------|
| Table 2-1: Typical Reservoir Compressibility..... | - 24 - |
|---|--------|

List of Figures

| | |
|---|---------|
| Figure 1: Interblock Flow | - 29 - |
| Figure 2: Straightline Method to Determine Aquifer Model (Havlena and Odeh) | - 33 - |
| Figure 3: Radial Aquifer | - 36 - |
| Figure 4: Linear Aquifer | - 37 - |
| Figure 5: Bottom Water Drive | - 38 - |
| Figure 6: Schematic of Aquifer Inflow Models | - 39 - |
| Figure 7: Typical Horizontal Wellbore Diagram | - 49 - |
| Figure 8: Control Volume for Pipe Flow | - 49 - |
| Figure 10: Wellbore Pressure Drop Path with Multiple Inflows | - 60 - |
| Figure 13: Schematic of Multiple Tanks with Aquifer | - 68 - |
| Figure 14: Schematic of Generalized Situation | - 71 - |
| Figure 16: Wellbore Production Rate for a Single Tank with No Aquifer Output | - 83 - |
| Figure 17: RU Flow Rate for a Single Tank with No Aquifer Output | - 84 - |
| Figure 18: RU Pressure for a Single Tank with No Aquifer Output | - 85 - |
| Figure 19: Pressure Depletion Rate for a Single Tank with No Aquifer Output .. | - 86 - |
| Figure 21: Wellbore Production for a Single Tank with Aquifer Output | - 90 - |
| Figure 22: RU Production for a Single Tank with Aquifer Output | - 91 - |
| Figure 23: RU Pressure for a Single Tank with Aquifer Output | - 92 - |
| Figure 24: Pressure Depletion for a Single Tank with Aquifer Output | - 93 - |
| Figure 26: Wellbore Production Rate for Two Non-Communicating Tanks with a Common Aquifer Output | - 97 - |
| Figure 27: RU Production for Two Non-Communicating Tanks with a Common Aquifer Output | - 98 - |
| Figure 28: RU Pressure for Two Non-Communicating Tanks with a Common Aquifer Output | - 99 - |
| Figure 29: Pressure Depletion for Two Non-Communicating Tanks with a Common Aquifer Output | - 100 - |
| Figure 31: Wellbore Production for Two Communicating Tanks with a Common Aquifer Output | - 104 - |
| Figure 32: RU Production for Two Communicating Tanks with a Common Aquifer Output | - 105 - |
| Figure 33: RU Pressure for Two Communicating Tanks with a Common Aquifer Output | - 106 - |
| Figure 34: Pressure Depletion for Two Communicating Tanks with a Common Aquifer Output | - 107 - |
| Figure 36: Wellbore Production for Three Non-Communicating Tanks without Aquifer Output | - 111 - |
| Figure 37: RU Production for Three Non-Communicating Tanks without Aquifer Output | - 112 - |

| | |
|--|---------|
| Figure 37: RU Production for Three Non-Communicating Tanks without Aquifer Output | - 112 - |
| Figure 38: RU Pressure for Three Non-Communicating Tanks without Aquifer Output | - 113 - |
| Figure 39: Pressure Depletion for Three Non-Communicating Tanks without Aquifer Output | - 114 - |
| Figure 41: Wellbore Production for Three Partially-Communicating Tanks with Partial-Aquifer Output | - 118 - |
| Figure 42: RU Production for Three Partially-Communicating Tanks with Partial-Aquifer Output | - 119 - |
| Figure 43: RU Pressure for Three Partially-Communicating Tanks with Partial-Aquifer Output | - 120 - |
| Figure 44: Pressure Depletion for Three Partially-Communicating Tanks with Partial-Aquifer Output | - 121 - |
| Figure 45: Total Production Rate Comparison | - 124 - |

List of Abbreviations, Nomenclature and Symbols

Abbreviations:

RU = Reservoir Unit

English Symbols with SI Units:

| | | |
|-----------|---|--------------------------------------|
| c | = Compressibility | $[\text{m}^3/\text{m}^3/\text{kPa}]$ |
| d | = Pipe diameter | $[\text{m}]$ |
| f | = Friction factor | |
| g | = Acceleration of gravity | $[\text{m}/\text{s}^2]$ |
| e_s | = Diameter of uncoated Gottingen sand | $[\text{m}]$ |
| h | = Net pay | $[\text{m}]$ |
| k | = Permeability, absolute | $[\text{m}^2]$ |
| k_{r_l} | = Relative permeability of phase l | $[\text{m}^2]$ |
| m | = Ratio of original gas in place to original oil in place at reservoir conditions | $[\text{rm}^3/\text{rm}^3]$ |
| r | = Radius | $[\text{m}]$ |
| t | = Time | $[\text{s}]$ |
| x | = Distance | $[\text{m}]$ |
| A_c | = Area of contact | $[\text{m}^2]$ |
| B | = Formation volume factor | $[\text{rm}^3/\text{sm}^3]$ |
| E_o | = Oil expansion | $[\text{m}^3/\text{m}^3]$ |
| F | = Net reservoir production | $[\text{m}^3]$ |
| G_i | = Original gas in place | $[\text{sm}^3]$ |

| | | |
|----------|---------------------------------|------------------------------------|
| J | = Transmissibility | $[\text{m}^3/\text{kPa}/\text{s}]$ |
| L | = Length | $[\text{m}^3]$ |
| N | = Original oil in place | $[\text{sm}^3]$ |
| N_p | = Cumulative oil production | $[\text{sm}^3]$ |
| P | = Pressure | $[\text{Pa}]$ |
| P_R | = Reservoir pressure | $[\text{Pa}]$ |
| P_{Ri} | = Initial reservoir pressure | $[\text{Pa}]$ |
| P_{wf} | = Wellbore flowing pressure | $[\text{Pa}]$ |
| Q | = Flow rate | $[\text{m}^3/\text{s}]$ |
| R_D | = Pipe Reynold's number | |
| R_s | = Solution gas oil ratio | $[\text{sm}^3/\text{sm}^3]$ |
| $S(P,t)$ | = Aquifer pressure function | $[\text{m}^3/\text{s}]$ |
| S | = Saturation | [fraction] |
| T | = Temperature | $[\text{K}]$ |
| U | = Aquifer constant | $[\text{m}^3/\text{Pa}/\text{s}]$ |
| V | = Volume | $[\text{m}^3]$ |
| W_e | = Cumulative water encroachment | $[\text{m}^3]$ |
| W_i | = Cumulative water injected | $[\text{m}^3]$ |
| W_p | = Cumulative water produced | $[\text{m}^3]$ |

Greek Symbols with SI Units:

| | | |
|----------|-----------------------|----------------------|
| γ | = Specific Gravity | [fraction] |
| μ | = Viscosity | [Pa s] |
| ρ | = Density | [kg/m ³] |
| σ | = Interfacial Tension | [mN/m] |
| τ | = Shear stress | [Pa] |
| ϕ | = Porosity | [fraction] |

Nomenclature:

Subscripts:

| | |
|-----|----------------------|
| i | = initial conditions |
| o | = oil |
| g | = gas |
| w | = water |
| f | = formation |
| s | = in solution |

List of Appendices

| | | |
|---|---------------------------------------|---------|
| A | Numerical Method Approach | - 138 - |
| B | Excel Main Calculation Sheet | - 142 - |
| C | Flowing Wellbore and Reservoir Solver | - 144 - |

1.0 Introduction

Subsurface petroleum engineering is a complex field involving many interdependencies between petroleum geology, petroleum phase behaviour, and multiphase flow.

In 1953, Uren defined a petroleum reservoir as follows:

“...a body of porous and permeable rock containing oil and gas through which fluids may move toward recovery openings under the pressure existing or that may be applied. All communicating pore space within the productive formation is properly a part of the rock, which may include several or many individual rock strata and may encompass bodies of impermeable and barren shale. The lateral expanse of such a reservoir is contingent only upon the continuity of pore space and the ability of the fluids to move through the rock pores under the pressure available.” (Uren, 1953)

Modern reservoir engineering relies heavily on simulation models to provide a reliable prediction of the subsurface petroleum system. An ideal reservoir simulation model is one that represents the main features and behavior of a real system, but is simple enough to perform calculations in an efficient manner.

Reservoir simulations may be either analytical or numerical. Analytical simulators are those whose equations are solved using algebraic or differential methods. Numerical simulators are those whose equations are so complex that they can only be solved by resolving to an acceptable, approximate solution using a numerical

algorithm. Both approaches have advantages and disadvantages and have been used successfully to approximate the behaviour of petroleum reservoirs.

Numerical simulation is data and computationally intensive and requires simplification of the natural system into approximations. Numerical simulation can, therefore, only provide a quasi-unique solution. It is often advantageous to use a more analytical, material balance approach to reservoir simulation.

The material balance approach is based fundamentally on analytical conservation for a zero dimensional system, meaning that no spatial variation within a lumped system is considered. The resulting balance, in the absence of transient effects can then be represented by an algebraic equation (Schilthuis, 1935 and Dake, 1978).

The material balance approach can provide insight on how reservoirs will behave at various stages, based primarily on fluid movement into or out of the system.

The material balance approach is particularly applicable in moderate to high transmissibility reservoirs where pressure transients within the lumped system are small.

The material balance approach does not have time directly within the equation, but time can be used in secondary calculations. An estimated production or injection forecast is imposed on the system to build a time component into the material balance, As such, the behaviour of the system can then influence the production forecast or a production forecast could influence the system behaviour.

As drilling technology has improved, and in an effort to improve the recovery efficiency of the available resource, the petroleum industry is trending toward more complicated well trajectories (i.e. horizontal, multilateral, geo-steered) with more complicated well completions (i.e. gravel pack, inflow/outflow control devices, commingled). These improvements in drilling technology have moved faster than the associated improvements in the simulation, resulting in results that do not have sufficient accuracy for advanced well designs. This has made traditional reservoir simulator partially obsolete because they are unable to represent the new complex wells accurately.

The widespread utilization of measure while drilling (MWD) for formation evaluation allows downhole data to be available real-time to the petroleum engineer. This provides the opportunity to use this data immediately, while still drilling the well. If we could take this data and perform reservoir and wellbore simulation in near real-time tremendous benefits could be realized in optimizing well design.

To simulate in near real-time, development of new models is required that are fast, accurate, and easy to use. This thesis is one possible approach to bridge this technology gap.

Standard modeling packages are cumbersome and difficult to adapt because they use complicated input files that are difficult to change because of a rigid simulation grid. They misrepresent the near wellbore by modeling the trajectory parallel to the grid regardless of the real trajectory and utilize relatively simple inflow models.

This thesis is a step forward in near real-time simulation as the proposed method is easy to implement and is capable of creating fast and accurate simulation models.

1.1 Scope of Research

It is important that complex reservoirs, wellbores, and completion technologies become unified into a single model that allows for future performance prediction and sensitivity assessments in an efficient and reliable manner, even while a well is being drilled. As such, a group of researchers at Memorial University of Newfoundland, Canada has been striving to develop the next generation of software, capable of meeting the challenge of today and tomorrow's oilfield development strategies.

One of the investigated approaches is to unify an advanced wellbore and near well reservoir model with analytical inflow relationships, to a dynamic material balance tank reservoir model. As proposed by Johansen, 2008, this work focuses on the dynamic material balance tank reservoir modeling and provides a solution to allow for efficient calculation of a flexible, multi-tank reservoir model.

The question that we investigated is can conventional material balance calculations be used to provide realistic long-term depletion forecasts in an efficient method that solves complex, multi-tank communicating, reservoir systems? Can these systems be integrated with advanced wellbore modeling techniques to increase the reliability of our predictions?

This research evaluates the integration of aquifer models, tank reservoirs, inter-tank transmissibility, well transmissibility, and wellbore performance into an integrated model that can be used to predict future well performance and conduct optimization evaluations. This work builds upon industry standard correlations and methods, but solves the integrated system using the Fourth-Order Runge-Kutta numerical method that has been shown to provide efficient and reliable results.

This work demonstrates the successful integration of aquifers, reservoir tanks, well inflow, and wellbore modeling into an integrated system that can quickly be used as a tool for investigating the petroleum systems. This work can form a fundamental module enabling the calculation of coupled wellbore and reservoir models needed for advanced completion technologies.

1.2 Thesis Outline

This body of work will present an overview of compressibility and transmissibility and a review of the traditional analytical aquifer modeling approach. A brief discussion of wellbore flow modeling is presented before building the general tank material balance approach. A series of demonstration cases is then presented before discussions on advantages and limitations of the described approach.

1.3 Literature Review

Schilthuis derived the general analytical material balance technique commonly used in today's oil and gas industry. Schilthuis described the inter relationship between reservoir pressure and production by using "active oil", "active free gas", aquifer influx, and the laboratory measured fluid properties. This provided a framework to conduct performance analysis of oil and gas reservoir from measured pressure and production data to determine the effectiveness of natural water drive and provide predictions of reservoir pressure under various operating conditions including water drive and gas re-injection (Schilthuis, 1935).

Van Everdingen and Hurst used Laplace transformations to develop solution to the unsteady state flow equation for the constant terminal pressure and the constant terminal rate cases. This built on previous work by Hurst showing that when the pressure history of a reservoir is known, that information can be used to calculate the water influx into the reservoir. These results can also be applied to well inflow when the diffusivity equation is obeyed (Van Everdingen and Hurst, 1949).

Carter and Tracy modified the work of Hurst and identified a method for calculating water influx behavior without using superposition. This was accomplished by assuming constant water influx rates are assumed, versus Hurst's constant oil production. This led to combining Schilthuis' material balance technique and allowing for an explicit step-wise calculation of pressure history. This resulted in a reduction in calculation time with acceptable results (Carter and Tracy, 1960).

Havlena and Oden used a straight line method to analyze the solution of the material balance equation. This method requires the plotting of one variable group against another where the resulting general shape of the plot is important. This method can be used to evaluate the drive mechanism, volumetrics of the connected reservoir, and the resultant sensitivity (Havlena and Odeh, 1963).

Fetkovich provided a simplification of previous aquifer influx methods that removed the need for superposition. He accomplished this by separating the water influx problem into a rate equation and a material balance equation making the concepts and calculation simple and easier to apply. This is now a very common method and has been demonstrated useful for long term predictions (Fetkovich, 1969).

Dake summarizes the zero dimensional material balance approach very well in his work where net underground withdrawal is a result of the expansion of oil and originally dissolved gases, expansion of gas cap gas, and a reduction in hydrocarbon pore volume due to the expansion of connate water and pore volume reduction. This generalized form includes effects from connate water expansion, rock expansion, free gas expansion, liberated gas expansion, oil expansion, aquifer influx, and fluid withdrawal. The general material balance equation is a "sophisticated version of the compressibility definition" where production is equal to the expansion of reservoir fluids (Dake, 1978).

Vogt and Wang added to the body of knowledge by presenting accurate formulas to calculate the material balance and water influx equation using the superposition

formula. They presented a generalized linear pressure formula with led to advantages for reservoirs with a variety of drive mechanisms (Vogt and Wang, 1987).

Butcher and Wanner provided a retrospective look at Runge-Kutta method with a focus on practical implementation of implicit methods, the use of linear and nonlinear stability analysis, and the theory and application of the methods (Butcher and Wanner, 1996).

Marques, Trevisan, and Suslick presented a comparative study of the classical method of influx calculation. This work showed the basic theory of four aquifer models and provided a comparison of total influx or water by the aquifer performance as a function of time with the van Everdingen and Hurst model used as comparison (Marques, Trevisan, and Suslick, 2007).

Petroleum Experts Ltd. has successfully implemented analytical material balance techniques in their Integrated Production Modeling software package to provide the classical reservoir engineer tool to analyze reservoir fluid dynamics using analytical techniques. Their methodology includes the ability to integrate multiple, zero-dimensional tanks by the use of the transmissibility concept (Petroleum Experts Ltd., 2009).

Penmatcha and Aziz presented a reservoir/wellbore model for horizontal wells (Penmatcha, 1999). The reservoir model consists of a transient, three-dimensional, uniform flux model, which, along with the principle of superposition in space and

time, is used to describe three-dimensional reservoir flow. The authors employed infinite and finite-conductivity well models, but the reservoir model is the uniform flux model of Babu and Odeh (Babu, 1989). This reservoir model has a no-flow boundary assumption and the well is represented as a line source.

Halliburton distributes the NETool program, which utilizes a steady-state numerical simulator for modeling of multiphase fluid flow inside the wellbore and the near wellbore region. The major drawback of this approach is the reservoir steady-state assumption, where time dependant changes in the far-field reservoir conditions are not incorporated into the system, thus allowing for only short-term applicability for the modeling results (Halliburton, 2010).

Recently, a new approach to combine transient well flow and reservoir flow modeling with a focus on advanced well completions has been developed. This model represents the first fully transient advanced well/reservoir flow model for three phase flow where co-current, countercurrent and cross flow may occur in different parts of the completion and reservoir simultaneously (Khorikov et al, 2010).

2.0 Background

2.1 Reservoir Units

Individual reservoir tanks and aquifers will be referenced as 'reservoir units' (RU) in this thesis. Each unit consists of a zero-dimensional system of a known initial volume, a known initial pressure, and a known total compressibility. Each reservoir unit (*RU*) will connect to other RUs in the model or to the wellbore through the means of a transmissibility, *J*, in the form:

$$Q = J(P_1 - P_2) \quad (2-1)$$

The concept of reservoir units, through communicating tanks, is a very useful concept that has many applications. Examples of potential applications include; faulted reservoirs with communicating or non-communicating faults, reservoirs with a connected aquifer, multiple reservoirs communicating through a common aquifer, a multi-layered reservoir of variable reservoir quality, a wellbore draining multiple reservoirs, or any system where an appreciable pressure gradient could exist.

2.2 Compressibility

Petroleum reservoirs are comprised of elements of variable degrees of compressibility. The sand grain compressibility is considered small in comparison with the pore compressibility in most petroleum reservoirs (Ahmed, 2006).

Typical values of the formation or rock (c_f), oil (c_o), water (c_w), and gas (c_g) compressibilities are shown as follows::

- Rock, $c_f = -12 \times 10^{-7}$ vol/vol/kPa
- Oil, $c_o = -40 \times 10^{-7}$ vol/vol/kPa
- Water, $c_w = -4 \times 10^{-7}$ vol/vol/kPa
- Gas, $c_g = -700 \times 10^{-7}$ vol/vol/kPa

One assumption is that compressibility is constant over the range of pressures being investigated. This is a reasonable assumption for oil, rock, and water but is not valid for gas. It is further assumed that one term, a total compressibility, c_t , is used in all calculations. Total compressibility is defined as the volume weighted average compressibility within a unit volume where S_o , S_w , and S_g are the oil, water and gas saturation within the pore space and calculated in Equation 2-2.

$$c_t = S_o c_o + S_w c_w + S_g c_g + c_f \quad (2-2)$$

Using the typical compressibilities listed above, [Table 2-1](#) illustrates the order of magnitude of total compressibilities for various reservoir types.

Table 2-1: Typical Reservoir Compressibility

| Reservoir Type | Oil Saturation | Water Saturation | Gas Saturation | Total Compressibility |
|--------------------|----------------|------------------|----------------|---------------------------|
| Aquifer | 0% | 100% | 0% | $\sim 10 \times 10^{-7}$ |
| Undersaturated Oil | 80% | 20% | 0% | $\sim 17 \times 10^{-7}$ |
| Gas | 0% | 20% | 80% | $\sim 150 \times 10^{-7}$ |

It is further assumed that the system will operate under isothermal conditions.

By definition, Equation 2-3 represents the formula describing the total compressibility of the system.

$$c_t = -\frac{1}{V} \left. \frac{\partial V}{\partial P} \right|_T \quad (2-3)$$

Equation 2-3 shows the relationship between the total compressibility, c_t , initial volume, V , isothermal change of volume, ∂V , and the isothermal change in pressure, ∂P .

In our application, the initial volume, V , represents the in-situ volume of fluid that is actively contributing to the system. The $\partial V / \partial P|_T$ term is the partial change in volume with respect to pressure under isothermal conditions. The total compressibility allows for the determination of the interrelationship between fluid

moving into or out of the system and the pressure of that system. A negative sign is imposed as a common convention so that the compressibility is a positive quantity.

2.3 Transmissibility

Flow in porous media is a very complex phenomenon that cannot be described explicitly, as flow through pipes or conduits can (Ahmed, 2006). This is a result of the vast number of potential flow paths, the dimensions of which are very difficult to measure and provide no clear-cut flow path. Understanding of the flow through porous medium has been learned through experimentation and analysis to establish laws (such as Darcy's law) and correlations.

Transmissibility is a term describing the ease by which fluids are able to move through the system. Transmissibility is analogous to conductivity in electric circuits.

The concept of transmissibility in reservoir engineering is a very useful concept. This concept can be applied to many areas of reservoir engineering, including movement of fluid from an aquifer to a reservoir, fluid movement within the reservoir, fluid movement between fault blocks, and fluid movement from the reservoir into or out of wellbores.

Transmissibility forms a fundamental building block in the modeling approach taken in this work, as will be explained in the Sections [2.3.12-3.1](#) to [2.3.32-3.3](#) below.

The unit of transmissibility is volume per pressure difference per time.

2.3.1 Aquifer Transmissibility

Aquifer transmissibility refers to the ability for fluid to flow between the aquifer and the reservoir. Several authors have published analytical techniques to approximate reservoir inflow including Schilthuis (Schilthuis, 1933), van Everdingen (van Everdingen et al., 1949), Fetkovich (Fetkovich, 1969), Carter-Tracy (Carter and Tracy., 1960), Hurst (Hurst, 1958), Vogt and Wang (Vogt and Wang, 1987), and Odeh (Odeh et al., 1965).

The fundamental building blocks of transmissibility are geometry (aquifer shape and volume), fluid mobility (permeability and viscosity), and connectivity (connected area). Aquifer transmissibility is for single-phase water flow.

Transmissibility equations exist for radial, linear, and bottom water drives under infinite acting, pseudo-steady-state, and steady-state flow regimes. The equations for several aquifer models and reservoir configurations are presented in Section [2.4.32.4.3](#).

2.3.2 Well Inflow Transmissibility

Well transmissibility refers to the ability for a fluid to flow between the wellbore and the reservoir.

A simplified approach has been taken for this work. This approach was to assign a single-phase constant transmissibility. This is a simplified assumption, and ignores relative permeability effects as well as transient flow periods.

The fundamental basis for the transmissibility is based on the Darcy's law, where:

$$Q = \frac{Kh}{\mu} \left(\frac{\Delta P}{\Delta x} \right) = J \left(\frac{\Delta P}{\Delta x} \right) \quad (2-4)$$

where

K = Absolute permeability

μ = viscosity

h = net pay

ΔP = Pressure change

Δx = Flow distance

and where J is the reservoir transmissibility, i.e.

$$J = \frac{kh}{\mu} \quad (2-5)$$

Many authors have published methods to calculate well inflow transmissibility under various reservoir situations, including Babu & Odeh, 1989, Standing, 1971, Vogel, 1968, Joshi, 1998, Furui, 2002, Peaceman, 1993, Peaceman 1995, and others. Any of these analytical models could be used to calculate the transmissibility for use in this model.

2.3.3 Inter-block Transmissibility

Transmissibility between communicating reservoir units is defined using the product of the average values of relative permeability, k_r , of phase l , absolute permeability K of each grid block at the interface between blocks, and cross-section area A_c of each grid block at the interface between blocks, divided by the production of the viscosity μ of phase l and the formation volume factor B_l of phase l in each reservoir unit, divided by the representative distance (Fanchi, 2006). This is also show in Equation 2-7.

The flow between blocks is graphically depicted in [Figure 1](#) in which the interblock transmissibility is determined by averaging the properties of the block which are exchanging fluid as well as the difference in pressure between the blocks.

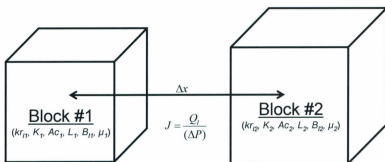


Figure 1: Interblock Flow

While different averaging techniques can be applied, we prefer a harmonic averaging technique for our scenario as show in Equation 2-6.

$$\frac{1}{\bar{K}} = \frac{1}{\Delta x_1 + \Delta x_2} \left(\frac{\Delta x_1}{K_1} + \frac{\Delta x_2}{K_2} \right) \quad (2-6)$$

Once the averaged properties are generated the inter-block transmissibility is given by Equation 2-7.

$$J = \frac{(\bar{k}_{r,i})(\bar{K})(\bar{A}_c)}{(\bar{L})(\bar{B}_i)(\bar{\mu}_i)} \quad (2-7)$$

where:

J = Transmissibility

$k_{r,i}$ = relative phase permeability

K = absolute rock permeability

B_i = formation volume factor

μ_l = viscosity

A_c = area of contact between blocks

L = representative distance between blocks

2.4 Aquifers

The petroleum industry's definition of an aquifer is a subterranean porous and permeable rock formation which may or may not be connected to the target hydrocarbon accumulation.

Aquifers can be used to provide source water for injection into a target reservoir, or as a disposal formation to inject brackish water.

When connected to a hydrocarbon formation, an aquifer will provide some degree of pressure support by movement of water into the hydrocarbon zone once a pressure differential exists. The result can have a positive or a negative impact on recovery dependant on the configuration of the system. An example is how a bottom-drive aquifer can often provide positive incremental recovery from an oil reservoir, but the same situation in a gas reservoir may reduce ultimate gas recovery due to trapped gas saturation in the water invaded zone or contribute to undesirable water coning.

Reliable characterization of an aquifer is fundamental to successful petroleum operations wherever aquifers play an appreciable role. However, extensive delineation of the aquifer is rarely done in practice, and characterization usually

involves seismic interpretation and material balance interpretation of measured reservoir pressures. As such, the impact of aquifers is often uncertain and can be a large source of error in forecasting future performance.

At its basic level, the aquifer is characterized by storage and by transmissibility. The storage of the reservoir is the connected pore volume. The transmissibility is the ability of the fluid contained in the aquifer to move, and is related to the connected shape, the aquifer permeability, saturation, the potential presence of a tar mat at the oil water contact, and the size of the aquifer. Transmissibility can be used to describe flow within the aquifer or flow from the aquifer to the hydrocarbon reservoir. We will focus on transmissibility between the aquifer and the hydrocarbon reservoir.

In a reservoir with a strong natural drive, a drop in the reservoir pressure, due to the production of fluids, causes the aquifer water to expand and flow into the reservoir or

$$\text{Water Influx} = \text{Aquifer Compressibility} \times \text{Initial Volume of Water} \times \text{Pressure Drop}$$

(Dake, 1978)

or

$$W_e = (c_w + c_f) W_i \Delta P \quad (2-8)$$

where

$$W_e = \text{Cumulative Water Influx}$$

c_w = water compressibility

c_f = formation compressibility

W_i = Initial water volume

ΔP = Pressure drop

Equation 2-8 assumes that change in pressure is transmitted instantaneously through the aquifer, which would only be valid in relatively small aquifers where the total water influx would be small anyways. In large aquifers the cumulative water influx would have a larger impact on reservoir performance, a time dependant water influx predictor is required as the pressure drop will not be immediately transmitted through the entire pore volume of the aquifer. This time dependant water influx predictor (i.e. a model) will be described in detail further in this section.

Using the technique of Havlena and Odeh (Havlena and Odeh, 1963 and 1964), the material balance under a simplified case (i.e. no gas cap) can be written in the form of

$$\frac{F}{E_o} = N + \frac{W_e}{E_o} \quad (2-9)$$

where

F = Net reservoir production, at downhole conditions

E_o = Oil expansion

N = Original oil in place, at surface conditions

W_e = Net aquifer influx assuming $B_w = 1.0$

The above equation is represented graphically in **Figure 2** where the aquifer model can be determined to be appropriate graphically.

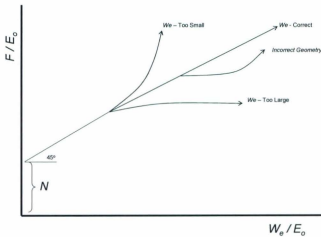


Figure 2: Straightline Method to Determine Aquifer Model (Havlena and Odeh)

The remainder of this section will describe in detail the methodology to apply aquifer models as well as the types available from current literature.

2.4.1 Aquifer Models

In general, equations for water influx can be written as a product of an aquifer constant and a pressure function. The aquifer constant is typically related to the shape and size of the aquifer, while the pressure function is typically related to the transmissibility between the aquifer and the reservoir (Van Everdingen et al, 1949).

$$We = U \bullet S(P,t) \quad (2-10)$$

where:

We = cumulative aquifer influx

U = aquifer constant

$S(P,t)$ = aquifer pressure function

There are numerous aquifer models and aquifer modeling techniques including small pot, radial, Schilthuis Steady State (Schilthuis, 1936), Hurst Steady State (Hurst 1958), Vogt-Wang (Vogt and Wang, 1987), Fetkovich Semi-Steady State (Fetkovich, 1969), Fetkovich Steady State (Fetkovich, 1969), and Carter-Tracy (Carter and Tracy, 1960). The most common methods, and those discussed in this paper, are the van-Everdingen and Hurst

(Van Everdingen et al, 1949), Fetkovich (Fetkovich, 1969), and Carter-Tracy aquifer modeling techniques (Carter and Tracy, 1960).

2.4.2 Aquifer Geometries

The physical size and shape of the aquifer is a principle unknown in petroleum engineering. Generally, the data collection on an aquifer is minimal and may only include an approximate bulk volume based on seismic interpretation. In addition to the geometry, the internal water pore volume and water mobility are also usually unknown.

During pre-production activities, the aquifer geometry and transmissibility is varied to perform a sensitivity analysis on the impact of the aquifer on the hydrocarbon recovery.

Then, during production activities the aquifer geometry and transmissibility is often used as a tuning parameter to match actual reservoir performance.

Irrespective of the stage of production, the subsurface engineers will make an assumption of the physical geometry of the connected aquifer. This shape influences the method by which the transmissibility and the resulting water influx are calculated.

Three commonly used geometries are shown in [Figure 3](#)[Figure-3](#), [Figure 4](#)[Figure-4](#), and [Figure 5](#)[Figure-5](#).

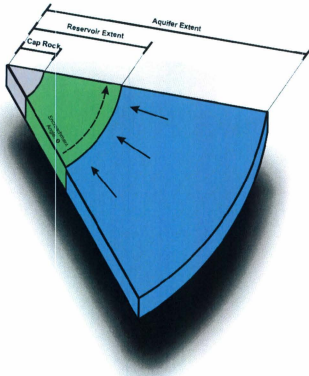


Figure 3: Radial Aquifer

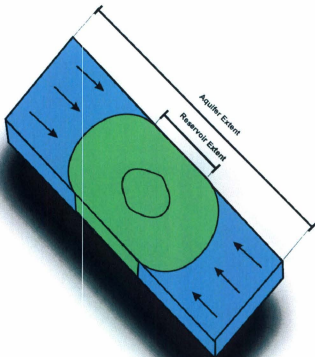


Figure 4: Linear Aquifer

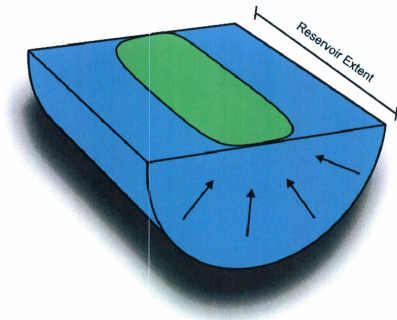


Figure 5: Bottom Water Drive

2.4.3 Aquifer Mathematical Models

Several authors have provided mathematical approximations to represent the effect of aquifers on reservoir performance. Three of the common models used today are the van Everdingen and Hurst, Fetkovich, and Carter-Tracy models. These will be reviewed in Sections 5.3.1 through Section 5.3.4.

The general approach to mathematical analysis of aquifers is to discretize the continuous inflow from the aquifer into steps to simplify the solution. These steps can be time- or pressure-based and will usually involve an average

pressure or flow rate during each calculation step. Some mathematical models use superposition while others simplify further and utilize the estimated current aquifer properties to calculate the next step.

The general approach is shown schematically in [Figure 6](#).

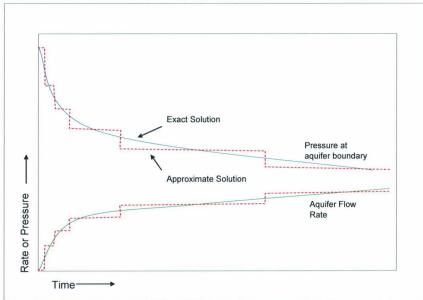


Figure 6: Schematic of Aquifer Inflow Models

As a general statement, the actual water influx from an aquifer has a large degree of uncertainty, particularly in the early production life of an oil or gas field. As such, the induced errors from simplification are likely to be within

the range of uncertainty around the properties of the aquifer themselves because the magnitude of water influx will be relatively small at early times.

2.4.3.1 van Everdingen and Hurst Aquifer Model

The authors (van Everdingen and Hurst, 1949) provided models for inflow from radial and linear aquifers acting as infinite, pseudo-steady state, and steady-state conditions.

This is performed by applying the Laplace transform to the diffusivity equation and with help from the superposition principle. The discretization of the continuous pressure curve allows for an approximate solution with:

$$W_e(t_{Dn}) = U \sum_{j=0}^{n-1} \Delta P_j W_D(t_{Dn} - t_{Dj}) \quad (2-11)$$

where:

$\Delta P_j = \bar{P}_j - \bar{P}_{j+1}$ is the change in average reservoir pressure during the j^{th} timestep, W_D is the accumulated dimensionless influx for a constant pressure drop at the aquifer boundary, $W_e(t_{Dn})$ is the cumulative dimensionless flow at the reservoir-aquifer boundary, and U is the influx constant of water into the aquifer.

The van Everdingen and Hurst model is based on the superposition principle resulting in additional computations are required because calculation results from previous steps are redone at each new time-step. This is because the value of We must be evaluated for the time and regime of the aquifer at the moment of interest. Simplifications have been proposed by Fetkovich and Carter-Tracy to streamline the computational effort.

There have been several variations to the original work of van Everdingen and Hurst by using slightly different pressure averaging techniques or approaches for determining fluid properties at each step, such as those presented by Odeh et. al. (Odeh, 1964) and Vogt (Vogt and Wang, 1987).

2.4.3.2 Fetkovich Aquifer Model

Fetkovich described a simplified method to calculate aquifer influx under a defined geometry and transmissibility (Fetkovich, 1971). This is an approximate model, but is useful as it does not require the application of the superposition principle as in the van Everdingen and Hurst model decreasing computational time (Marques, 2007). Fetkovich's original work addressed pseudo-steady state flow regimes for water flow from the aquifer to the reservoir.

The basic equations for the Fetkovich model stem from the generalized rate equation (assuming Darcy Law), Equation 2-12, and the aquifer material balance for constant compressibility, Equation 2-13.

$$q_w = J_q (\bar{P} - P_{wf}) \quad (2-12)$$

where q_w is the average water influx rate, J_q is the aquifer to reservoir transmissibility, \bar{P} is the average initial aquifer pressure, and P_{wf} is the average pressure at the aquifer / reservoir interface.

$$\bar{P} = - \left(\frac{P_i}{W_{ei}} \right) W_e + P_i \quad (2-13)$$

Fetkovich proposed a step-wise solution to the calculation, where the flow of fluid from the aquifer to the reservoir is a function of time and the pressure drop at the boundary. This yields the following general form.

$$\Delta W_{e_n} = \frac{W_e}{P_i} (\bar{P}_{(n-1)} - \bar{P}_{wfn}) \left\{ 1 - e^{-\left[\frac{(q_w)_{lim}}{W_e} \right] N_n} \right\} \quad (2-14)$$

where the average aquifer pressure at time = n is

$$\bar{P}_{n-1} = - \left(\frac{P_i}{W_{ei}} \right) W_e + P_i \quad (2-15)$$

and the average pressure at the aquifer boundary at time = n is

$$\bar{P}_{wf} = \frac{P_{wf(n-1)} + P_{wf(n)}}{2} \quad (2-16)$$

The flow rate from the aquifer to the reservoir was determined when Fetkovich applied the transmissibility concept where the aquifer productivity index, J_w , is a function of the rock and fluid properties of the system, the contact area, and the aquifer shape.

2.4.3.3 Fetkovich Aquifer Model Rate Equations

Using the concept of transmissibility, we next present several formulas that can be used to determine the rate of water influx. This is important, particularly for large aquifers, where the pressure drop due to production is not instantly transmitted through the entire aquifer.

The pseudo-steady state radial model:

$$W_{ei} = \pi(C_f + C_w)A_e r_w^2 (R_d^2 - 1)h\phi\rho_0 / (360.0 * 5.615) \quad (2-17)$$

$$J = \frac{0.007084 k_f h}{360.0 \mu_w (\log_2(R_d) - 0.75)} \quad (2-18)$$

where:

A_e = Encroachment angle, degrees

R_w = Reservoir radius, ft

h = Reservoir thickness, ft

R_d = Outer/inner radius ratio

P_0 = Initial aquifer pressure, psia

J = Transmissibility

c_f = Formation compressibility, 1/psi

c_w = Water compressibility, 1/psi

ϕ = Aquifer porosity

The pseudosteady-state linear model:

$$L_a = \frac{10^6 V_a}{W_r h \phi} \quad (2-19)$$

$$W_{ei} = 10^6 (C_f + C_w) V_a P_0 / 5.615 \quad (2-20)$$

$$J = \frac{0.00127 k_a h W_r}{\mu_w L_a} \quad (2-21)$$

where:

V_a = Aquifer volume, sq ft

W_r = reservoir width, ft

h = reservoir thickness, ft

k_a = aquifer permeability, mD

The pseudosteady-state bottom drive model:

$$L_a = \frac{10^6 V_a}{\pi_w^2 \phi} \quad (2-22)$$

$$W_{ei} = 10^6 (C_f + C_w) V_a P_0 / 5.615 \quad (2-23)$$

$$J = \frac{0.00127 k_a \pi_w^2}{\mu_w L_a} \quad (2-24)$$

where:

V_a = aquifer volume, ft³

R_w = reservoir radius, ft

k_a = aquifer permeability, mD

For the steady-state aquifer inflow models, W_{ei} is the same as the pseudosteady-state inflow models except that the transmissibility is calculated differently.

The steady-state radial model:

$$J = \frac{0.00708 A_a k_a h}{360.0 \mu_w (\log_2 R_d)} \quad (2-25)$$

The steady-state linear model:

$$J = \frac{0.0038 W_a h W_r}{\mu_a L_a} \quad (2-26)$$

The steady-state bottom drive model:

$$J = \frac{0.00381 k_a r_w^2}{\mu_a L_a} \quad (2-27)$$

2.4.3.4 Carter-Tracy Aquifer Model

The Carter-Tracy Aquifer model is similar to Fetkovich in that it does not require the application of the superposition principle (Carter, 1960). The model covers any flow geometry, as long as the solution for the dimensionless pressure as a function of time is known. This is a popular model due to its ease for computational application and general usefulness as it applies dimensionless variables.

This model is an extension of the Hurst model that presented an approach to the aquifer model that eliminated superposition calculations (Hurst, 1958). The elimination of superposition calculation was achieved by adopting the assumption of constant water influx rates for finite time periods. This allows for simplification of the entire influx history into a "fictitious" constant rate thereby eliminating the need for the superposition calculations and provides a reasonable approximation that can be used with the Schilthuis form of the material balance equation.

The Carter-Tracy model approximates the cumulative aquifer influx W_e by

$$W_e(t_{Dj}) = W_e(t_{Dj-1}) + \left(\frac{U \Delta P(t_{Dj}) - W_e(t_{Dj-1}) P_D'(t_{Dj})}{P_D(t_{Dj}) - t_{Dj-1} P_D'(t_{Dj})} \right) (t_{Dj} - t_{Dj-1}) \quad (2-28)$$

where:

U = the aquifer influx constant

$\Delta P(t_{Dj}) = P_i - P(t_{Dj})$ = the pressure drop at the boundary

$t_{Dj} = \alpha(t_r - t_0)$

$P_D(t_{Dj})$ = the dimensionless pressure in the producing boundary of an aquifer producing under constant flow

The Carter-Tracy aquifer model only assumes radial inflow, so the following equations are applied.

$$\alpha = \frac{2.309 k_a}{365.25 \phi \mu_w (C_f + C_w)_w^2} \quad (2-29)$$

$$U = \frac{1.119 A_e \phi h (C_f + C_w)_w^2}{360.0} \quad (2-30)$$

where:

k_a = Aquifer permeability, mD

R_w = reservoir radius, ft

A_e = encroachment angle, degrees

h = reservoir thickness, ft

2.5 Wellbore Flow Modeling

Reservoir fluids are transported to surface by means of a wellbore. Wellbores used in the petroleum industry have many variants, but are most commonly circular. This allows the wellbore to be modeled as flow in pipes, where there are many potential arrangements possible. For this body of work, steady-state single-phase flow has been assumed. Future studies could expand this work to include multi-phase flow where required.

Figure 7 depicts a typical flowing well arrangement for a horizontal well completed with a production liner.

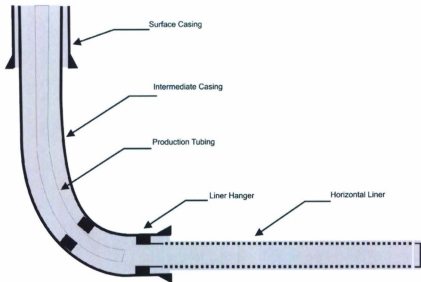


Figure 7: Typical Horizontal Wellbore Diagram

For a fixed segment of pipe, a control volume can be determined and is shown graphically in [Figure 8](#) ~~Figure-8~~.

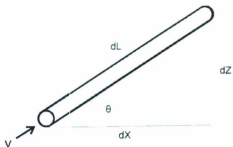


Figure 8: Control Volume for Pipe Flow

Applying the principle of conservation of mass, momentum, and energy it is possible to calculate pressure and temperature changes with distance for this system.

Applying the conservation of mass steady-state flow in a fixed segment of pipe means that the mass in minus the mass out, equals mass accumulation or

$$\frac{\partial p}{\partial t} + \frac{\partial(pv)}{\partial L} = 0 \quad (2-31)$$

where:

p = pressure

v = volume

L = length of pipe segment

t = time

With our assumption of steady-state flow where mass accumulation does not occur, Equation 2-31 can be reduced to

$$\frac{\partial(pv)}{\partial L} = 0 \quad (2-32)$$

If we apply conservation of momentum (Newton's first law) to wellbores it would require that the sum of all forces on the fluids would equate to the rate of momentum

out, minus the rate of momentum in, plus the rate of momentum accumulation in a fixed segment of pipe. The conservation of momentum is depicted as

$$-\frac{\partial p}{\partial L} - \tau \frac{\pi d}{A} - pg \sin \theta = \frac{\partial(pv)}{\partial t} + \frac{\partial(pv^2)}{\partial L} \quad (2-33)$$

where:

g = gravitational constant, m/s/s

τ = shear stress, pa

d = pipe diameter, m

A = pipe flow area, m²

Equation 2-32 and Equation 2-33 can be combined under the steady-state flow assumption and solved for the pressure gradient within the fluid resulting in the following equation.

$$\frac{dp}{dL} = -\tau \frac{\pi d}{A} - pg \sin \theta - pv \frac{dv}{dL} \quad (2-34)$$

Equation 2-34 shows that the steady-state pressure gradient within a flowing well is made up of three components, and in general

$$\left(\frac{dp}{dL}\right)_{total} = \left(\frac{dp}{dL}\right)_{friction} + \left(\frac{dp}{dL}\right)_{hydrostatic} + \left(\frac{dp}{dL}\right)_{acceleration} \quad (2-35)$$

The dominant term in Equation 2-35 is the hydrostatic head, or pressure gradient caused by elevation change and can often represent more than 80% of the total pressure gradient and is more dominant with more liquid. The secondary term is the frictional component which becomes more significant with higher flowing velocity. The minor term is the acceleration (or kinetic energy) component which is usually negligible but can be significant in low pressure systems with a compressible fluid, such as low pressure gas wells.

2.5.1 Frictional Pressure Drop

A pressure drop can be caused by frictional forces between the fluid and the wall as well as between fluid and fluid moving at different velocities.

The Darcy-Weisbach equation expresses the pressure loss in a piping system. (Darcy, 1858 and Weisbach, 1872).

$$\frac{\Delta p}{\rho} = f \left(\frac{L}{D} \right) \left(\frac{V^2}{2g_c} \right) \quad (2-36)$$

where:

f = apparent friction factor

L = length, m

D = diameter, m

ρ = density, kg/m³

ΔP = pressure drop, kPa

g_c = acceleration of gravity, m/s²

V = velocity, m/s

The friction factor, in general, is a function of the pipe Reynolds number and the relative roughness (Benedict, 1980). Flow in pipes can either be laminar ($Re < 2000$), turbulent ($Re > 2100$), or in the transition zone between laminar and turbulent (Benedict, 1980).

2.5.1.1 Laminar Flow in Smooth Pipes

In the years 1839 and 1846, Hagen and Poiseuille, working independently, showed that the Darcy-Weisbach generalized pressure drop equation provided an expression for the laminar friction factor (f_L) when equated with their results:

$$f_L = \frac{64}{Re} \quad (2-37)$$

2.5.1.2 Turbulent Flow in Smooth Pipes

Blasius plotted friction factor against Reynolds number for smooth circular pipes at pipe Reynolds numbers up to 10^5 and obtained an empirical

relationship shown in Equation 2-38 which was later shown to be independent of the fluid type and compressibility (Blasius, 1911).

$$f_{Blasius} = 0.3164R_D^{-1/4} \quad (2-38)$$

R_D = Reynold's Pipe Number, dimensionless

Prandtl built upon this work to generalize the friction factor into terms of a full cross-sectional area pipe flow shown in Equation 2-39 (Prandtl, 1933).

$$\frac{1}{\sqrt{f_s}} = 2 \log(R_D \sqrt{f_s}) - 0.8 \quad (2-39)$$

2.5.1.3 Turbulent Flow in Fully Rough Pipes

Friction factor is independent of wall roughness in laminar flow, but roughness is of fundamental importance in turbulent pipe flow.

Nikuradse, building upon Darcy's earlier work, performed a series of experiments on artificially roughened pipes and generated a relative roughness scale. Von Karman analyzed this data and generated Equation 2-40 for friction in a fully rough pipe in turbulent flow (Benedict, 1980).

$$\frac{1}{\sqrt{f_R}} = 2 \log\left(\frac{R}{e_s}\right) + 1.74 \quad (2-40)$$

where:

R = radius of uncoated pipe, m

e_s = diameter of uncoated Gottingen sand, m

f_r = friction factor for rough pipes

2.5.1.4 Transition between Smooth and Rough Pipes

The empirical equations for friction factor in both smooth and in rough pipes break down in the transition zone between laminar and turbulent flow regimes.

Colebrook developed a mathematical function which gave a transitional curve between the smooth and rough pipes equations by combining the two expressions for friction factor into a single equation which he confirmed through experimentation. The equation is presented in Equation 2-41 (Colebrook, 1938).

$$\frac{1}{\sqrt{f_r}} = 1.74 - 2 \log \left(2 \frac{e}{D} + \frac{18.7}{R_D \sqrt{f_r}} \right) \quad (2-41)$$

The Haaland equation can be used to solve directly for friction factor in a full-flowing circular pipe. This equation is an approximation of the Colebrook

equation but provides an explicit formula for rough pipes. The equation is shown in Equation 2-42 (Haaland, 1983).

$$\frac{1}{\sqrt{f}} = -1.8 \log \left[\left(\frac{\varepsilon/D}{3.7} \right)^{1.11} + \frac{6.9}{\text{Re}} \right] \quad (2-42)$$

2.5.1.5 Moody Plot

Moody provided a convenient to use composition plot which included all flow regimes of interest. This includes the straight line laminar friction factor curve, the smooth pipe turbulent friction factor curve, the fully rough turbulent friction factor curves, and the transition friction factors and is a good tool for implicit determination of Darcy friction factor (Moody, 1944).

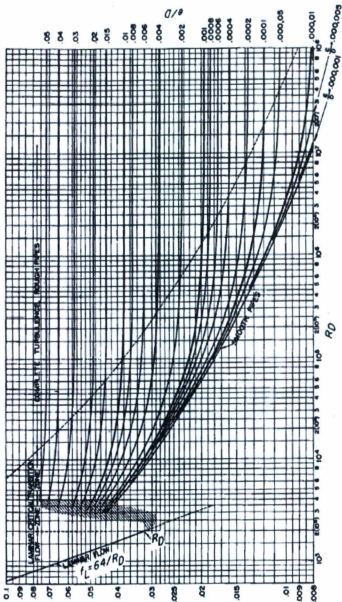


Figure 9: Friction Factor Map (after Moody, 1944)

2.5.1.6 Chen Correlation

Chen's correlation is being used to evaluate the friction factor for this work and is shown in Equation 2-43. This correlation has an explicit form and gives similar accuracy as the Moody plot (Chen, 1979).

$$\frac{1}{\sqrt{f_F}} = -4 \times \log \left[\frac{\varepsilon}{3.7065} - \frac{5.0452}{N_{Re}} \log \left(\frac{\varepsilon^{1.1098}}{2.8257} + \left(\frac{7.149}{N_{Re}} \right)^{0.8981} \right) \right] \quad (2-43)$$

where:

$$\varepsilon = \delta/d$$

δ = absolute roughness of the pipe wall, ft

d = pipe diameter, ft

2.5.2 Hydrostatic Pressure Drop

Hydrostatic pressure drop is a function of gravitation pull, height, and density. For our control volume shown in [Figure 8](#) this equates to

$$\Delta P = \rho g \cos \theta L \quad (2-44)$$

2.5.3 Kinematic Pressure Drop

Kinematic (or acceleration) pressure drop is caused by changes in velocity of the fluid, particularly in highly compressible fluids. This is of particular concern with gas wells near surface, flow across chokes, and where there are changes in production tubing size. For our scenario, the Bernoulli equation can represent the kinematic pressure drop.

$$\Delta P = \frac{\rho \Delta u^2}{2} \quad (2-45)$$

2.5.4 Total Pressure Drop

Where the assumption of single phase pressure drop in isothermal conditions is made, Equation 2-46 is being used which corresponds to the simplified flow schematic presented in [Figure 10](#) ~~Figure-10~~ which is used to calculate the bottomhole flowing pressure as a function of depth along the wellbore. The bottomhole flowing pressure is used to determine the amount of inflow from the corresponding reservoir unit.

If we integrate Equation 2-35 for the length of the production tubing requiring evaluation, the following pressure drop equation results and can be used directly in calculations:

$$\Delta P = P_1 - P_2 = \rho g \cos \theta L + \rho \frac{\Delta u^2}{2} + \frac{f_F \rho u^2 L}{D} \quad (2-46)$$

where:

f_F = Darcy friction factor

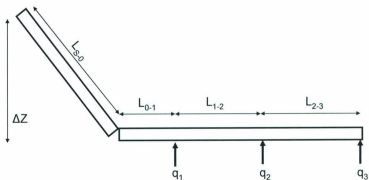


Figure 10: Wellbore Pressure Drop Path with Multiple Inflows

3.0 Mathematical Development of Analytical Tank Modeling

The fundamental building block of the analytical tank approach is the reservoir unit (RU). Each unit could represent any section of the petroleum reservoir system that is desired to be modeled. The RU could represent the entire reservoir including the aquifer, the entire reservoir excluding the aquifer, a portion of the reservoir, a fault block, a specific stratigraphic layer, or a section of a stratigraphic layer such as a reservoir simulator grid block. The only requirement is that the reservoir statics and flow properties can be reasonably approximated for use in engineering calculations. This will likely limit this approach to the modeling of large, defined sections of the reservoir, such as fault blocks, or to the modeling of the reservoir as a whole.

As discussed in Sections [2.22-2](#) and [2.32-3](#), the performance of a RU is controlled by two concepts, the compressibility and the inter-tank transmissibility. The two equations are restated below:

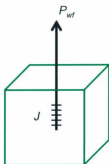


Figure 11: Schematic of Single Tank

$$c_i = -\frac{1}{V_i} \frac{dV}{dP} \quad (3-1)$$

$$q_w = J(P_r(t) - P_{wf}(t)) \quad (3-2)$$

Through substitution and combination, Equation 3-1 and Equation 3-2 yields the following system of equations of the form:

$$\frac{dP_r}{dt} = -\frac{J}{c_b V_i} (P_r(t) - P_{wf}(t)) \quad (3-3)$$

$$\frac{dV}{dt} = J(P_r(t) - P_{wf}(t)) \quad (3-4)$$

Equation 3-3 and Equation 3-4 can be integrated using an exact solution or by using a numerical method such as the 4th Order Runge-Kutta method to determine the pressure and cumulative production at any time, t . This method is formulated in Appendix A.

3.1 Exact Solution of Single Tank Modeling

As the single tank modeling solution is relatively simple, it is straight forward to determine an exact solution using Equation 3-3 and Equation 3-4. This is accomplished by integration using an initial boundary condition as described below.

The initial boundary conditions can be applied, namely:

$$\text{At } t = 0; P = P_i \text{ and at } t = t, P = P(t)$$

The steps of integration are as follows:

$$\int_{P_i}^P \frac{dP}{(P_r(t) - P_{wf})} = -\frac{J}{c_b V_i} \int_0^t dt \quad (3-5)$$

$$\ln \left(\frac{P_r(t) - P_{wf}}{P_i - P_{wf}} \right) = -\frac{J}{c_b V_i} (t - 0) \quad (3-6)$$

$$\left(\frac{P_r(t) - P_{wf}}{P_i - P_{wf}} \right) = e^{-\frac{J}{c_b V_i} t} \quad (3-7)$$

Therefore,

$$P_r(t) = P_{wf} + (P_i - P_{wf}) e^{-\frac{J}{c_b V_i} t} \quad (3-8)$$

where $P_r(t)$ is the average reservoir pressure at any time, t .

The other important and related equation is to evaluate the change in volume as a function of time. In this case, the following boundary conditions are applied

At $t = 0$, $P = P_i$ and $V_o = 0$ where V = cumulative oil produced at time, t .

At $t = t$, $P = P(t)$ and $V_o = V(t)$

hence:

$$\int_0^V dV = J \int_0^t (P - P_{wf}) dt \quad (3-9)$$

From Equation 3-9:

$$V(t) = J(P - P_{wf}) \int_0^t e^{-\frac{J}{cV_r} t} dt \quad (3-10)$$

$$V(t) = J(P - P_{wf}) \left[-\frac{cV_r}{J} e^{-\frac{J}{cV_r} t} \right]_0^t \quad (3-11)$$

$$V(t) = cV_r(P - P_{wf}) \left(1 - e^{-\frac{J}{cV_r} t} \right) \quad (3-12)$$

Equation 3-12 represents the cumulative fluid production at time t from the reservoir unit. These two equations (Equation 3-8 and Equation 3-12) are very useful for modeling reservoir units and form the basis for all types of reservoir simulations. They describe, within a defined reservoir volume, the relationship between total system compressibility and pressure. They also describe the drive mechanism and volume of fluid movement between defined volumes as a function of time.

These two equations can be expanded to encompass many reservoir units, with multiple inter-related communication pathways and multiple production pathways. If representative reservoir volumes, total compressibility, and inter-tank transmissibility can be reasonably defined, these two equations can form the basis of a full-field reservoir model system that can be practically used to evaluate many real-life reservoir development situations.

The following sections outline this concept will be illustrated and defined starting from the simplest system and ending with a generalized system.

3.2 Single Tank with Aquifer

A single RU can be linked with an aquifer by the use of interblock transmissibility.

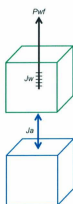


Figure 12: Schematic of Single Tank with Aquifer

This will yield the following system of equations where the subscript a relates to the aquifer, r relates to the reservoir, and w relates to the wellbore as depicted in Figure 12.

$$c_{br} = -\frac{1}{V_r} \frac{dV}{dP} \quad (3-13)$$

$$q_w = J_w(P_r(t) - P_{wf}(t)) \quad (3-14)$$

$$c_{ba} = -\frac{1}{W_i} \frac{dW}{dP} \quad (3-15)$$

$$q_{a-r} = J_a(P_a(t) - P_r(t)) \quad (3-16)$$

Where the subscript $a-r$ relates to flow between the aquifer and the reservoir unit. By combination of Equation 3-13 through Equation 3-16:

$$\frac{dP_r}{dt} = \frac{J_a}{c_a W_i} (P_a(t) - P_r(t)) - \frac{J_w}{c V_i} (P_r(t) - P_{wf}(t)) \quad (3-17)$$

$$\frac{dV_w}{dt} = J(P_r(t) - P_{wf}(t)) \quad (3-18)$$

$$\frac{dW_a}{dt} = J_a(P_a(t) - P_r(t)) \quad (3-19)$$

Equation 3-17 through Equation 3-19 can be integrated to determine the reservoir pressure and cumulative aquifer influx and reservoir production at any time t . Again, this is an initial value problem, but the determination of the exact solution becomes more difficult to calculate and a numerical integration method becomes a more useful approach.

3.3 Multiple Tanks with Multiple Aquifers

The fundamental building blocks and the associated equations allow for any number of RUs can be connected. This system of tanks can be interconnected in any manner desired, and simply requires a connection transmissibility and the associated tank reservoir properties.

Figure 13 is an example of three RUs connected to two aquifers with a variety of connections. This demonstrates some of the functionality of the proposed methodology by allowing for flow from one tank into more than one other tank. This could represent one aquifer communicating to multiple reservoirs.

This also demonstrates the possibility for local refinement where necessary, such as near the production well to provide more accuracy for well inflow modeling.

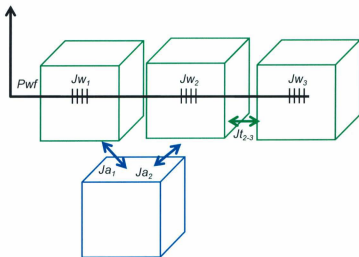


Figure 13: Schematic of Multiple Tanks with Aquifer

This will yield the following system of equations

Reservoir Unit #1:

$$c_{br1} = -\frac{1}{V_{r1}} \frac{dV}{dP} \quad (3-20)$$

$$q_{w1} = J_{w1}(P_{r1}(t) - P_{wf1}(t)) \quad (3-21)$$

Reservoir Unit #2:

$$c_{br2} = -\frac{1}{V_{r2}} \frac{dV}{dP} \quad (3-22)$$

$$q_{w2} = J_{w2}(P_{r2}(t) - P_{wf2}(t)) \quad (3-23)$$

Reservoir Unit #3

$$c_{br3} = -\frac{1}{V_{r3}} \frac{dV}{dP} \quad (3-24)$$

$$q_{w3} = J_{w3}(P_{r3}(t) - P_{wf3}(t)) \quad (3-25)$$

$$q_{r2-3} = J_{r2-3}(P_{r3}(t) - P_{r2}(t)) \quad (3-26)$$

Aquifer Unit #1

$$c_{ba} = -\frac{1}{W_i} \frac{dW}{dP} \quad (3-27)$$

$$q_{a-r1} = J_{a-r1}(P_a(t) - P_{r1}(t)) \quad (3-28)$$

$$q_{a-r2} = J_{a-r2}(P_a(t) - P_{r2}(t)) \quad (3-29)$$

Through combination of Equations 3-20 through 3-29 the pressure and flow behaviour of the system can be solved simultaneously by the following equations:

$$\frac{dP_a}{dt} = -\frac{J_{a-1}}{c_{b_a} W_i} (P_a(t) - P_{r1}(t)) - \frac{J_{a-2}}{c_{b_a} W_i} (P_a(t) - P_{r2}(t)) \quad (3-30)$$

$$\frac{dP_{r1}}{dt} = -\frac{J_{a-1}}{c_{b_{r1}} V_{r1}} (P_{r1}(t) - P_a(t)) - \frac{J_{w1}}{c_{b_{r1}} V_{r1}} (P_{r1}(t) - P_{wf1}(t)) \quad (3-31)$$

$$\frac{dP_{r2}}{dt} = -\frac{J_{a-2}}{c_{b_{r2}} V_{r2}} (P_{r2}(t) - P_a(t)) - \frac{J_{w2}}{c_{b_{r2}} V_{r2}} (P_{r2}(t) - P_{wf2}(t)) - \frac{J_{i2-3}}{c_{b_{r2}} V_{r2}} (P_{r2}(t) - P_{r3}(t)) \quad (3-32)$$

$$\frac{dP_{r3}}{dt} = -\frac{J_{w3}}{c_{b_{r3}} V_{r3}} (P_{r3}(t) - P_{wf3}(t)) - \frac{J_{i2-3}}{c_{b_{r3}} V_{r3}} (P_{r3}(t) - P_{r2}(t)) \quad (3-33)$$

Equations 3-30 through 3-33 are the set of equations that can be integrated to determine the reservoir pressure and cumulative aquifer influx and reservoir production at any time t . Again, this is an initial value problem, but the determination of the exact solution becomes impossible to calculate and a numerical integration method must be used.

3.4 Generalized Formulas

Any number of RUs can be connected to any number of perforated sections by using the fundamental building blocks and the associated equations. This system of tanks can be interconnected in any manner desired and simply requires a connection transmissibility and the associated tank reservoir properties.

This is important as the set of ordinary differential equations can be expanded to meet the requirements of the desired model, providing flexibility in the construction of the model to match the complexity of the situation.

In a general sense, the following equations can be used to describe any system with any combination, as shown in [Figure 14](#) ~~Figure-14~~.

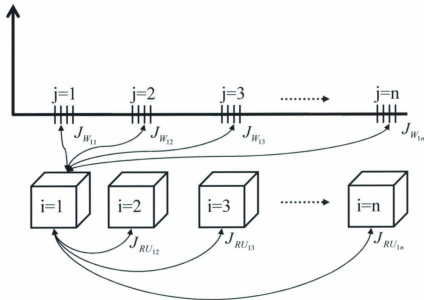


Figure 14: Schematic of Generalized Situation

The generalized flow equations are shown in Equation 3-34 through Equation 3-35.

$$c_{b_{RUi}} = -\frac{1}{V_{RUi}} \frac{dV}{dP} \quad (3-34)$$

$$q_{RU_a} = \sum_{k=1}^{k=n} \sum_{i=1}^{i=n} [J_{RU_a} (P_{RU_i}(t) - P_{RU_k}(t))] \quad (3-35)$$

The generalized flow equation between the reservoir units and the perforations is shown in Equation 3-36.

$$q_{w_j} = \sum_{j=1}^{j=n} \sum_{i=1}^{i=n} [J_{w_j} (P_{RU_i}(t) - P_{w_j}(t))] \quad (3-36)$$

where i is the specified flow from the reservoir unit, J is the specified well perforation, and J_{w_j} is the transmissibility between the specific RU and the specific well perforation.

The generalized reservoir unit pressure is shown in Equation 3-37.

$$\left. \frac{dP_{RU_i}}{dt} \right|_{i=1}^{i=n} = \sum_{k=1}^{k=n} \sum_{j=1}^{j=n} \left[-\frac{J_{RU_{ik}}}{c_{b_i} V_i} (P_{RU_i}(t) - P_{RU_j}(t)) \right] + \sum_{j=1}^{j=n} \sum_{i=1}^{i=n} \left[-\frac{J_{w_{ij}}}{c_{b_i} V_i} (P_{RU_i}(t) - P_{w_j}(t)) \right] \quad (3-37)$$

where $J_{RU_{jk}}$ is the specific transmissibility between RU i and k , c_{b_i} is the specific compressibility of RU i , and V_i is the specific volume of RU i , and $J_{w_{ij}}$ represents the specific transmissibility between RU i and well segment j .

The generalized reservoir unit production rate is shown in Equation 3-38.

$$\left. \frac{dV_{RU_i}}{dt} \right|_{t=1}^{t=n} = \sum_{k=1}^{k=n} \sum_{i=1}^{i=n} \left[-J_{RU_k} \left(P_{RU_k}(t) - P_{RU_i}(t) \right) \right] + \sum_{j=1}^{j=n} \sum_{i=1}^{i=n} \left[-J_{w_j} \left(P_{RU_i}(t) - P_{w_j}(t) \right) \right] \quad (3-38)$$

where J_{RU_k} is the specific transmissibility between RU k and i , P_{RU_k} is the pressure of RU k , P_{RU_i} is the pressure of RU i , and J_{w_j} is the transmissibility between well segment j and RU i , P_{w_j} is the wellbore pressure at wellbore segment j .

3.5 Assumptions

In developing this work, several simplifying assumptions have been made including constant compressibility, isothermal conditions, and single phase flow.

Constant compressibility was assumed as the focus was on oil reservoirs and aquifers. This assumption means that, in the pressure range calculated, a single value is able to represent the compressibility. This assumption could be considered valid for rock, water, and under saturated oil reservoir across moderate pressure variation. This assumption can be removed by redefining compressibility from Equation 3-39.

$$pV = ZnRT \quad (3-39)$$

where:

n = number of moles

p = pressure, kPa

T = temperature, K

V = volume, m^3

Z = compressibility factor

Equation 3-40, the real gas law, can be re-arranged to:

$$V = \frac{ZnRT}{P} = nRT \frac{Z}{P} \quad (3-40)$$

Then

$$\frac{dV}{dP} = nRT \frac{d\left(\frac{Z}{P}\right)}{dP} \quad (3-41)$$

$$\frac{dV}{dP} = nRT \left[\frac{1}{P} \frac{dZ}{dP} - Z \frac{1}{P^2} \right] \quad (3-42)$$

$$\frac{dV}{dP} = \frac{ZnRT}{P} \frac{1}{Z} \frac{dZ}{dP} - \frac{ZvRT}{P} \frac{1}{P} \quad (3-43)$$

By re-arranging and substitution with the real gas law:

$$\frac{1}{V} \frac{dV}{dP} = \frac{P}{ZnRT} \left[\frac{ZnRT}{P} \frac{1}{Z} \frac{dZ}{dP} - \frac{ZvRT}{P} \frac{1}{P} \right] = \frac{1}{Z} \frac{dZ}{dP} - \frac{1}{P} \quad (3-44)$$

or in terms of compressibility:

$$c = -\frac{1}{V} \frac{dV}{dP} = \frac{1}{P} - \frac{1}{Z} \left(\frac{dZ}{dP} \right)_T \quad (3-45)$$

Another assumption in this these are isothermal conditions. This assumption is valid for the large majority of operating reservoirs and is considered valid except in certain situations. To remove this assumption, an energy balance model could be added for each tank. In this scenario, the temperature calculations would be executed after the fluid motion calculation making the temperature calculations decoupled from the mass transfer. Convection and conduction could be incorporated along with fluid mixing models. Incorporation of non-isothermal conditions is beyond the scope of this thesis but would be relatively simple to add at a later date.

Single phase flow was assumed in this thesis. This simplification was made as multi-phase flow was not necessary to demonstrate the usefulness of a coupled tank-well

modeling. The reason this assumption was made was because the structure of all reservoir models use a similar approach. The fundamental flow equation in all models is:

$$Q = J(\Delta P) \quad (3-46)$$

To handle multiple phases the concept of relative permeability is applied. Relative permeability is an extension of Darcy's Law where the effective permeability of one phase is impacted by the saturation of a second phase such that the relative permeability of one phase is equal to or less than the total effective permeability.

$$Q_T = Jk_{ro}(\Delta P) + Jk_{rw}(\Delta P) + Jk_{rg}(\Delta P) \quad (3-47)$$

In the simulation world, two relative permeability curves are typically used; the gas-liquid relative permeability and the oil-water relative permeability. The models will determine the amount of gas flow from one block to the other using the gas-liquid relative permeability and the gas and liquid saturation. Independently the models will determine the oil and water saturations and the resultant oil and water relative permeability to determine the relative volumes of oil and water flowing. Together, the gas, oil, and water flow rates are calculated.

3.6 Other Scenarios

Fundamentally, any number of aquifers, reservoir units, wellbore connections, and inter-tank transmissibilities can be evaluated. The limitation is only limited to the computing time and the engineering usefulness of the granularity of the calculations.

This provides the ability to model a variety of situations such as faulted reservoirs with communicating or non-communicating faults, reservoirs with a connected aquifer, multiple reservoirs communicating through a common aquifer, a multi-layered reservoir of variable reservoir quality, a wellbore draining multiple reservoirs, or any system where an appreciable pressure gradient could exist.

3.7 Limits of Methodology Discussion

No limit to the applicability of this approach has been encountered by this author. However, demonstration of this was not possible as the implementation and execution of the computer code was conducted in Microsoft Excel with has limited capabilities to conduct this investigation. The two scenarios that were going to be investigated were to determine the maximum number of tanks that could be calculate and the maximum number of tanks connected to the wellbore.

3.7.1 Maximum Number of Tanks

The generalized set of equations described above could be used to evaluate the maximum number of tank that could be evaluated simultaneously. As mentioned above, this could not be completed due to limitations imposed by Excel.

However, there is reason to believe that the number of tanks could be substantial. This is because systems of ordinary differential equations are very well behaved because all variable change smoothly and the variation in communication between tanks is handle through the index with each tank being homogenous.

It is also known that numerical solutions to systems of ordinary differential equations generally do not experience stability problems when generalized. Therefore, numerical difficulties are not expected to be significant. If increase accuracy is desired, a multi-step method could be implemented. (Atkinson, Han, 2004).

3.7.2 Maximum Number of Wellbore to Tank Connections

The generalized set of equations described above could be used to evaluate the maximum number of tank that could be calculated to the wellbore. This would have allowed for evaluation of the length of the well. As mentioned above, this could not be completed due to limitations imposed by Excel.

The length of a production well is important because it allows for capital efficient exploitation of additional reservoir volume. However, pressure drop along the well will eventually limit this exploitation as the minimum predicted well bore pressure approached the reservoir pressure; as friction along the length of the well will limit the drawdown.

The present model can play an important role in determining the optimal well length. It could also be used to evaluate technologically complex wellbore designs such as wells equipped with inflow control devises, outflow control devises, selective perforations, and downhole isolation packers.

3.8 Numerical Approach

The 4th Order Runge-Kutta (RK) Method was chosen to solve the series of ordinary differential equations generated by the system of units being evaluated in the modeling. The 4th Order is the most common of the RK methods because of the ease of use and high numerical order. This method also provides a high degree of accuracy in an efficient manner.

The numerical approach is described in detail in the Appendix.

4.0 Results of Demonstration Cases

A series of demonstration cases are investigated below to evaluate the flexibility and usefulness of the 4th Order Runge-Kutta method to a system of first-order differential equations. The cases were designed to show increasing levels of complexity and inter-tank dependence.

All of the cases evaluated consist of a single wellbore producing from one or more tanks where some or all of the tanks are connected to an aquifer. This allows for the investigation of how fluids and pressures interact between the reservoir units and the wellbore to show the impact of transmissibility, connected pore volume, and aquifer pressure support.

The demonstration cases start with the simplest system of only one drawdown point, one tank, and no aquifer. The most complicated case involve three partially communicating tanks with partial aquifer support.

The cases all assume that production is controlled by a target initial rate, then use a minimum flowing tubing head pressure for control.

An input sheet is presented for each scenario along with the output plus a discussion of the results. A comparison of the results is also provided.

4.1 Single Tank, No Aquifer

This case represents a production well draining a single tank without support of an aquifer. In this case, the pressure of the tank is only a function of the production rate.

The input assumptions are presented in Figure 15 [Error! Reference source not found](#), with the output presented in [Figure 16](#) through [Figure 19](#).

Scenario Schematic:

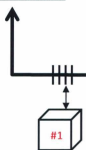


Figure 15: Single Tank with No Aquifer Output

Fluid Properties:

| | |
|-----------------------------|------------------------------------|
| Viscosity | 0.5 mPas |
| Density | 980 kg/m ³ |
| Formation Volume Factor | 1 rm ³ /sm ³ |
| Relative Phase Permeability | 0.7 Relative to Air |

Reservoir Unit Properties:

| | Tank #1 | Tank #2 | Tank #3 | Tank #4 (Aquifer) |
|--------------------------|------------|-----------|------------|----------------------------|
| Initial Pressure | 30,000 | 30,000 | 30,000 | 30,000 kPa |
| Initial Bulk Volume | 5.0E+07 | 4.0E+07 | 6.0E+07 | 1.5E+08 rm ³ |
| Initial Fluid Saturation | 100% | 100% | 100% | 100% |
| Initial Porosity | 20% | 20% | 20% | 20% |
| Initial Pore Volume | 10,000,000 | 8,000,000 | 12,000,000 | 30,000,000 rm ³ |
| Rock Compressibility | 1.20E-06 | 1.25E-06 | 1.00E-06 | 1.20E-06 /kPa |
| Fluid Compressibility | 4.00E-07 | 4.00E-07 | 4.00E-07 | 4.00E-07 /kPa |
| Total Compressibility | 1.60E-06 | 1.65E-06 | 1.40E-06 | 1.60E-06 /kPa |
| Permeability | 10 | 10 | 10 | 1 mD |

Intertank Properties:

| Flow Area (m ³) | Tank #1 | Tank #2 | Tank #3 | Tank #4 (Aquifer) |
|-----------------------------|---------|---------|---------|-------------------|
| Tank #1 | - | - | - | - |
| Tank #2 | - | - | - | - |
| Tank #3 | - | - | - | - |
| Tank #4 | - | - | - | - |

| Distance (m) | Tank #1 | Tank #2 | Tank #3 | Tank #4 |
|--------------|---------|---------|---------|---------|
| Tank #1 | - | 800 | 800 | 800 |
| Tank #2 | 800 | - | 800 | 800 |
| Tank #3 | 800 | 800 | - | 800 |
| Tank #4 | 800 | 800 | 800 | - |

| Transmissibility (m ³ /d/kPa) | Tank #1 | Tank #2 | Tank #3 | Tank #4 |
|--|---------|---------|---------|---------|
| Tank #1 | - | - | - | - |
| Tank #2 | - | - | - | - |
| Tank #3 | - | - | - | - |
| Tank #4 | - | - | - | - |

Wellbore Properties:

| | |
|----------------|----------|
| Tubing ID | 0.219 m |
| Pipe Roughness | 0.046 mm |

| Transmissibility (m ³ /d/kPa) | Tank #1 | Tank #2 | Tank #3 |
|--|---------|---------|---------|
| Jw | 0.20 | - | - |

| | Tank #1 | Tank #2 | Tank #3 |
|------------|---------|---------|---------|
| Depth (m3) | 1,000 | 1,025 | 1,050 |

Control Conditions:

| | |
|----------------------------|------------------------|
| Minimum THP | 4000 kPa |
| Minimum Rate | 200 m ³ /d |
| Target Rate | 6000 m ³ /d |
| Max Time Step | 15 days |
| Max Pressure Drop per Step | 50 kPa |
| Minimum Time Step | 5 days |

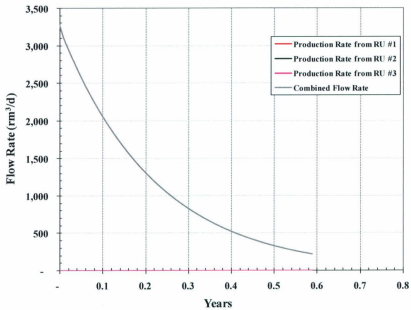


Figure 16: Wellbore Production Rate for a Single Tank with No Aquifer Output

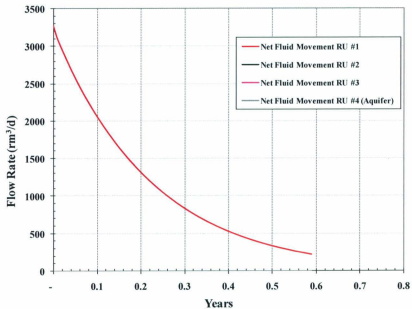


Figure 17: RU Flow Rate for a Single Tank with No Aquifer Output

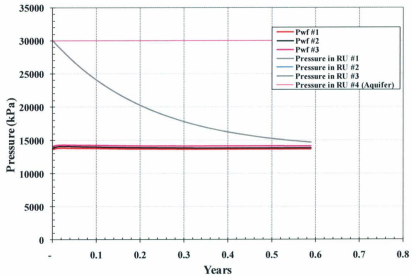


Figure 18: RU Pressure for a Single Tank with No Aquifer Output

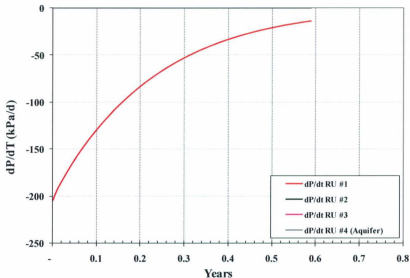


Figure 19: Pressure Depletion Rate for a Single Tank with No Aquifer Output

4.1.1 Discussion of Results

This case represents a straight depletion of the reservoir unit. The depletion of the reservoir unit occurs very quickly as would be the case for a small, slightly compressible reservoir. This scenario could represent a small, highly under saturated oil reservoir or a limited volume water source well.

Figure 16 demonstrates that with the assumed productivity, the target production rate of 6000 m³/d is not achieved and the drawdown rate is dictated by the minimum allowable tubing head pressure.

Figure 16 and Figure 17 have identical flow rates, which is exactly as expected as all of the fluid entering the well is being produced from the single tank.

4.2 Single Tank, With Aquifer

This case represents a production well draining a single tank with the support of an aquifer with 3 times the initial bulk volume. In this case, the pressure of the tank is a function of the production rate as well as the net influx from the aquifer.

The input assumptions are presented in [Error! Reference source not found](#), Figure 20 with the output presented in [Figure 21](#) through [Figure 24](#).

Scenario Schematic:

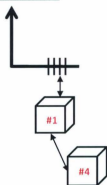


Figure 20: Single Tank with Aquifer Output

Fluid Properties:

| | |
|-----------------------------|-----------------------------------|
| Viscosity | 0.5 mPas |
| Density | 980 kg/m ³ |
| Formation Volume Factor | 1 m ³ /sm ³ |
| Relative Phase Permeability | 0.7 Relative to Air |

Reservoir Unit Properties:

| | Tank #1 | Tank #2 | Tank #3 | Tank #4 (Aquifer) |
|--------------------------|------------|-----------|------------|----------------------------|
| Initial Pressure | 30,000 | 30,000 | 30,000 | 30,000 kPa |
| Initial Bulk Volume | 5.0E+07 | 4.0E+07 | 6.0E+07 | 1.5E+08 rm ³ |
| Initial Fluid Saturation | 100% | 100% | 100% | 100% |
| Initial Porosity | 20% | 20% | 20% | 20% |
| Initial Pore Volume | 10,000,000 | 8,000,000 | 12,000,000 | 30,000,000 rm ³ |
| Rock Compressibility | 1.20E-06 | 1.25E-06 | 1.00E-06 | 1.20E-06 /kPa |
| Fluid Compressibility | 4.00E-07 | 4.00E-07 | 4.00E-07 | 4.00E-07 /kPa |
| Total Compressibility | 1.60E-06 | 1.65E-06 | 1.40E-06 | 1.60E-06 /kPa |
| Permeability | 10 | 10 | 10 | 1 mD |

Intertank Properties:

| Flow Area (m ²) | Tank #1 | Tank #2 | Tank #3 | Tank #4 (Aquifer) |
|-----------------------------|---------|---------|---------|-------------------|
| Tank #1 | - | - | - | 800 |
| Tank #2 | - | - | - | - |
| Tank #3 | - | - | - | - |
| Tank #4 | 800 | - | - | - |

| Distance (m) | Tank #1 | Tank #2 | Tank #3 | Tank #4 |
|--------------|---------|---------|---------|---------|
| Tank #1 | - | 800 | 800 | 800 |
| Tank #2 | 800 | - | 800 | 800 |
| Tank #3 | 800 | 800 | - | 800 |
| Tank #4 | 800 | 800 | 800 | - |

| Transmissibility (rm ³ /d/kPa) | Tank #1 | Tank #2 | Tank #3 | Tank #4 |
|---|---------|---------|---------|---------|
| Tank #1 | - | - | - | 0.22 |
| Tank #2 | - | - | - | - |
| Tank #3 | - | - | - | - |
| Tank #4 | 0.22 | - | - | - |

Wellbore Properties:

| | |
|----------------|----------|
| Tubing ID | 0.219 m |
| Pipe Roughness | 0.046 mm |

| | | | |
|---|---------|---------|---------|
| Transmissibility ($\text{m}^3/\text{d}/\text{kPa}$) | Tank #1 | Tank #2 | Tank #3 |
| Jw | 0.20 | - | - |

| | | | |
|------------|---------|---------|---------|
| | Tank #1 | Tank #2 | Tank #3 |
| Depth (m3) | 1,000 | 1,025 | 1,050 |

Control Conditions:

| | |
|----------------------------|----------------------------|
| Minimum THP | 4000 kPa |
| Minimum Rate | 200 m^3/d |
| Target Rate | 6000 m^3/d |
| Max Time Step | 15 days |
| Max Pressure Drop per Step | 50 kPa |
| Minimum Time Step | 5 days |

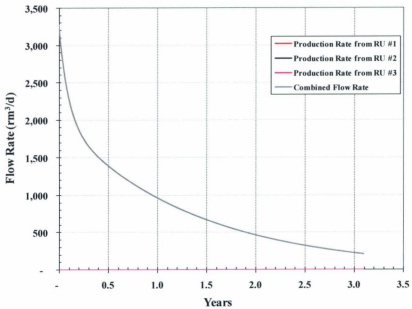


Figure 21: Wellbore Production for a Single Tank with Aquifer Output

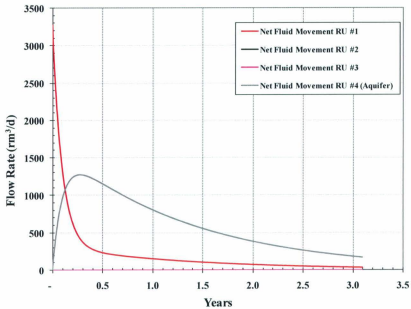


Figure 22: RU Production for a Single Tank with Aquifer Output

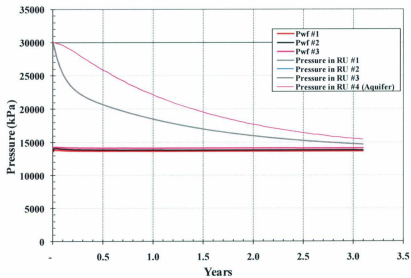


Figure 23: RU Pressure for a Single Tank with Aquifer Output

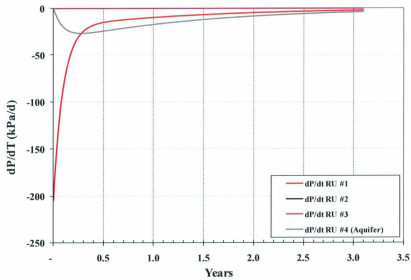


Figure 24: Pressure Depletion for a Single Tank with Aquifer Output

4.2.1 Discussion of Results

This case represents a depletion of the reservoir unit #1 plus the influx from reservoir unit #4 (aquifer). With the volume and the compressibility assumed, the depletion of the reservoir unit occurs slower than without the aquifer, and the cumulative production volume is larger.

[Figure 21](#) confirms the expectation that with aquifer influx, the overall decline will be reduced while the initial productivity is still not improved enough to meet the production target of 6000 m³/d.

[Figure 26](#) and [Figure 28](#) demonstrate the interplay between wellbore transmissibility and aquifer transmissibility. These figures show that the production rate into the well is greater than the aquifer influx causing the pressure to continue to deplete in RU#1 until the well is shut-in due to hitting the minimum production rate of 200 m³/d.

4.3 Two Non-Communicating Tanks, With Common Aquifer

This case represents a production well draining two non-communicating reservoir units, both supported by a common aquifer with three times the initial bulk volume of reservoir unit #1. In this case, the pressures of both tanks are functions of the cumulative production volume as well as the net influx from the aquifer.

The input assumptions are presented in Figure 25 [Error! Reference source not found.](#) with the output presented in [Figure 26](#) [Figure-26](#) through [Figure 29](#) [Figure-29](#).

Scenario Schematic:

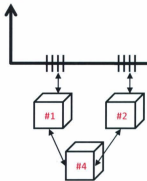


Figure 25: Two Non-Communicating Tanks with Common Aquifer Input

Fluid Properties:

| | |
|-----------------------------|------------------------------------|
| Viscosity | 0.5 mPas |
| Density | 980 kg/m ³ |
| Formation Volume Factor | 1 rm ³ /sm ³ |
| Relative Phase Permeability | 0.7 Relative to Air |

Reservoir Unit Properties:

| | Tank #1 | Tank #2 | Tank #3 | Tank #4 (Aquifer) |
|--------------------------|------------|-----------|------------|----------------------------|
| Initial Pressure | 30,000 | 30,000 | 30,000 | 30,000 kPa |
| Initial Bulk Volume | 5.0E+07 | 4.0E+07 | 6.0E+07 | 1.5E+08 rm ³ |
| Initial Fluid Saturation | 100% | 100% | 100% | 100% |
| Initial Porosity | 20% | 20% | 20% | 20% |
| Initial Pore Volume | 10,000,000 | 8,000,000 | 12,000,000 | 30,000,000 rm ³ |
| Rock Compressibility | 1.20E-06 | 1.25E-06 | 1.00E-06 | 1.20E-06 /kPa |
| Fluid Compressibility | 4.00E-07 | 4.00E-07 | 4.00E-07 | 4.00E-07 /kPa |
| Total Compressibility | 1.60E-06 | 1.65E-06 | 1.40E-06 | 1.60E-06 /kPa |
| Permeability | 10 | 10 | 10 | 1 mD |

Intertank Properties:

| Flow Area (m ²) | Tank #1 | Tank #2 | Tank #3 | Tank #4 (Aquifer) |
|-----------------------------|---------|---------|---------|-------------------|
| Tank #1 | - | - | - | 800 |
| Tank #2 | - | - | - | 500 |
| Tank #3 | - | - | - | - |
| Tank #4 | 800 | 500 | - | - |

| Distance (m) | Tank #1 | Tank #2 | Tank #3 | Tank #4 |
|--------------|---------|---------|---------|---------|
| Tank #1 | - | 800 | 800 | 800 |
| Tank #2 | 800 | - | 800 | 800 |
| Tank #3 | 800 | 800 | - | 800 |
| Tank #4 | 800 | 800 | 800 | - |

| Transmissibility (m ² /d/kPa) | Tank #1 | Tank #2 | Tank #3 | Tank #4 |
|--|---------|---------|---------|---------|
| Tank #1 | - | - | - | 0.22 |
| Tank #2 | - | - | - | 0.14 |
| Tank #3 | - | - | - | - |
| Tank #4 | 0.22 | 0.14 | - | - |

Wellbore Properties:

| | |
|----------------|----------|
| Tubing ID | 0.219 m |
| Pipe Roughness | 0.046 mm |

| Transmissibility (m ² /d/kPa) | Tank #1 | Tank #2 | Tank #3 |
|--|---------|---------|---------|
| Jw | 0.20 | 0.30 | - |

| | Tank #1 | Tank #2 | Tank #3 |
|------------|---------|---------|---------|
| Depth (m3) | 1,000 | 1,025 | 1,050 |

Control Conditions:

| | |
|----------------------------|------------------------|
| Minimum THP | 4000 kPa |
| Minimum Rate | 200 m ³ /d |
| Target Rate | 6000 m ³ /d |
| Max Time Step | 15 days |
| Max Pressure Drop per Step | 50 kPa |
| Minimum Time Step | 5 days |

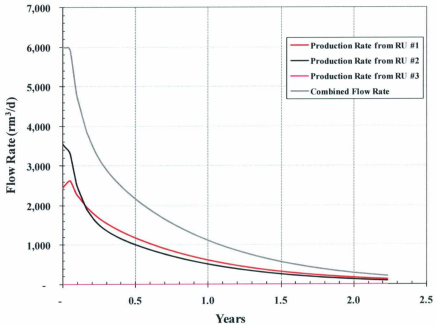


Figure 26: Wellbore Production Rate for Two Non-Communicating Tanks with a Common Aquifer Output

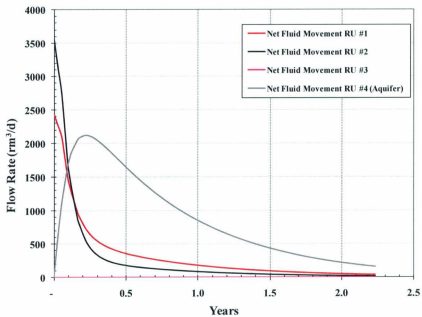


Figure 27: RU Production for Two Non-Communicating Tanks with a Common Aquifer Output

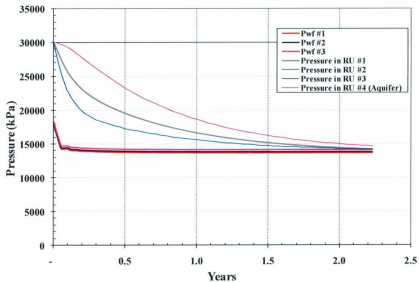


Figure 28: RU Pressure for Two Non-Communicating Tanks with a Common Aquifer Output

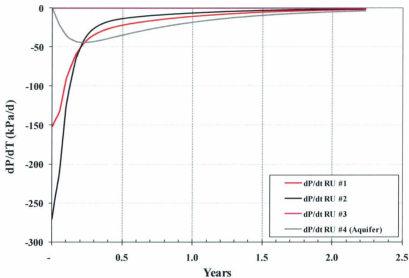


Figure 29: Pressure Depletion for Two Non-Communicating Tanks with a Common Aquifer Output

4.3.1 Discussion of Results

This case demonstrates that the solving routine can solve for the depletion of both tanks connected to a common aquifer. The results show the relative contribution from each tank is a function of the well transmissibility, the aquifer to reservoir unit transmissibility, the depth of the perforations, the compressibility and initial pore volume differences between the two reservoir units.

The maximum production target of $6000 \text{ m}^3/\text{d}$ is achieved in this scenario for a short period of time, as shown in [Figure 26](#). Initially, the production rate from

RU# is greater than RU#1 due to higher transmissibility and reservoir pressure. This is only temporary as greater pressure depletion in RU#2, shown in [Figure 28](#) and [Figure 29](#), results in the production from RU#1 be the main contributor.

The aquifer contributes to both RU#1 and RU#2, but greater pressure support is provided to RU#1, shown in [Figure 28](#). This aligns with the greater transmissibility between the aquifer and RU#1.

4.4 Two Communicating Tanks, With Common Aquifer

This case represents a production well draining two communicating reservoir units, both supported by a common aquifer with 3 times the initial bulk volume of reservoir unit #1. In this case, the pressures of both tanks are functions of the relative production rate into the wellbore, as well as the net influx of fluid from the common aquifer. So, at each calculated time step the pressure of the individual reservoir units changes depending on how much support is being provided by the aquifer as well as how much production is entering the well.

The total production target from the well has been doubled to account for more production capacity from the two tanks.

The input assumptions are presented in [Figure 30](#) [Error! Reference source not found.](#) with the output presented in [Figure 31](#) through [Figure 34](#).

Scenario Schematic:

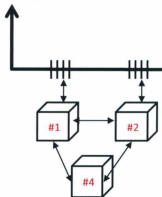


Figure 30: Two Communicating Tanks with Common Aquifer Input

Fluid Properties:

| | |
|-----------------------------|-----------------------------------|
| Viscosity | 0.5 mPas |
| Density | 980 kg/m ³ |
| Formation Volume Factor | 1 m ³ /sm ³ |
| Relative Phase Permeability | 0.7 Relative to Air |

Reservoir Unit Properties:

| | Tank #1 | Tank #2 | Tank #3 | Tank #4 (Aquifer) | |
|--------------------------|------------|-----------|------------|-------------------|-----------------|
| Initial Pressure | 30,000 | 30,000 | 30,000 | 30,000 | kPa |
| Initial Bulk Volume | 5.0E+07 | 4.0E+07 | 6.0E+07 | 1.5E+08 | rm3 |
| Initial Fluid Saturation | 100% | 100% | 100% | 100% | |
| Initial Porosity | 20% | 20% | 20% | 20% | |
| Initial Pore Volume | 10,000,000 | 8,000,000 | 12,000,000 | 30,000,000 | rm ³ |
| Rock Compressibility | 1.20E-06 | 1.25E-06 | 1.00E-06 | 1.20E-06 | /kPa |
| Fluid Compressibility | 4.00E-07 | 4.00E-07 | 4.00E-07 | 4.00E-07 | /kPa |
| Total Compressibility | 1.60E-06 | 1.65E-06 | 1.40E-06 | 1.60E-06 | /kPa |
| Permeability | 10 | 10 | 10 | 1 | mD |

Intertank Properties:

| Flow Area (m ²) | Tank #1 | Tank #2 | Tank #3 | Tank #4 (Aquifer) |
|-----------------------------|---------|---------|---------|-------------------|
| Tank #1 | - | 150 | - | - |
| Tank #2 | 150 | - | - | - |
| Tank #3 | - | - | - | - |
| Tank #4 | - | - | - | - |

| Distance (m) | Tank #1 | Tank #2 | Tank #3 | Tank #4 |
|--------------|---------|---------|---------|---------|
| Tank #1 | - | 800 | 800 | 800 |
| Tank #2 | 800 | - | 800 | 800 |
| Tank #3 | 800 | 800 | - | 800 |
| Tank #4 | 800 | 800 | 800 | - |

| Transmissibility (m ³ /d/kPa) | Tank #1 | Tank #2 | Tank #3 | Tank #4 |
|--|---------|---------|---------|---------|
| Tank #1 | - | 0.23 | - | - |
| Tank #2 | 0.23 | - | - | - |
| Tank #3 | - | - | - | - |
| Tank #4 | - | - | - | - |

Wellbore Properties:

| | |
|----------------|----------|
| Tubing ID | 0.219 m |
| Pipe Roughness | 0.046 mm |

| Transmissibility (m ³ /d/kPa) | Tank #1 | Tank #2 | Tank #3 |
|--|---------|---------|---------|
| J _w | 0.20 | 0.30 | - |

| | Tank #1 | Tank #2 | Tank #3 |
|------------|---------|---------|---------|
| Depth (m3) | 1,000 | 1,025 | 1,050 |

Control Conditions:

| | |
|----------------------------|------------------------|
| Minimum THP | 4000 kPa |
| Minimum Rate | 200 m ³ /d |
| Target Rate | 6000 m ³ /d |
| Max Time Step | 15 days |
| Max Pressure Drop per Step | 50 kPa |
| Minimum Time Step | 5 days |

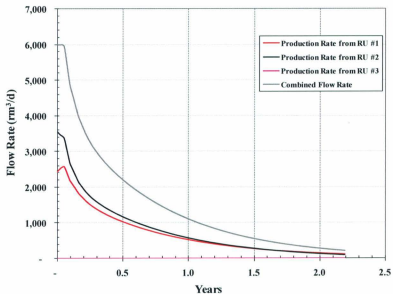


Figure 31: Wellbore Production for Two Communicating Tanks with a Common Aquifer Output

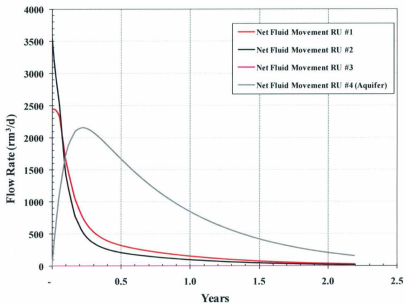


Figure 32: RU Production for Two Communicating Tanks with a Common Aquifer Output

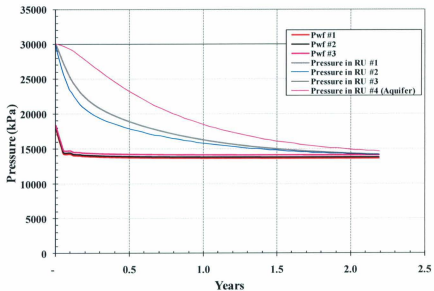


Figure 33: RU Pressure for Two Communicating Tanks with a Common Aquifer Output

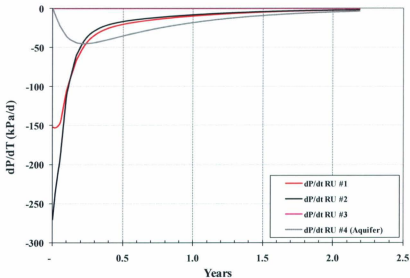


Figure 34: Pressure Depletion for Two Communicating Tanks with a Common Aquifer Output

4.4.1 Discussion of Results

This case demonstrates that the solving routine can solve for the depletion of both tanks connected to a common aquifer. The results show the relative contribution from each tank is a function of the well transmissibility, the aquifer to reservoir unit transmissibility, the inter-tank transmissibility, the depth of the perforations, the compressibility and initial pore volume differences between the two reservoir units.

The results show that the difference in pressure in reservoir unit #1 and reservoir unit #2 is reduced relative to the previous scenario as shown in [Figure 33](#). This

is a result of fluids being able to move between the RUs. In a real-world scenario, this may allow for assessment of fault transmissibility.

4.5 Three Non-Communicating Tanks, Without Aquifer

This case represents a production well draining three non-communicating reservoir units, not supported by a common aquifer. In this case, the pressure of the three tanks is a function of the relative production rate as well as initial pore volume and compressibility only.

The input assumptions are presented in Figure 35 Error! Reference source not found. with the output presented in Figure 36 Figure-36 through Figure 39 Figure-39.

Scenario Schematic:

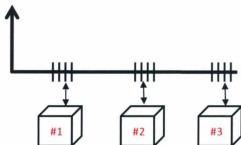


Figure 35: Three Non-Communicating Tanks without Aquifer Input

Fluid Properties:

| | |
|-----------------------------|-----------------------------------|
| Viscosity | 0.5 mPas |
| Density | 980 kg/m ³ |
| Formation Volume Factor | 1 m ³ /sm ³ |
| Relative Phase Permeability | 0.7 Relative to Air |

Reservoir Unit Properties:

| | Tank #1 | Tank #2 | Tank #3 | Tank #4 (Aquifer) |
|--------------------------|------------|-----------|------------|---------------------------|
| Initial Pressure | 30,000 | 30,000 | 30,000 | 30,000 kPa |
| Initial Bulk Volume | 5.0E+07 | 4.0E+07 | 6.0E+07 | 1.5E+08 m ³ |
| Initial Fluid Saturation | 100% | 100% | 100% | 100% |
| Initial Porosity | 20% | 20% | 20% | 20% |
| Initial Pore Volume | 10,000,000 | 8,000,000 | 12,000,000 | 30,000,000 m ³ |
| Rock Compressibility | 1.20E-06 | 1.25E-06 | 1.00E-06 | 1.20E-06 /kPa |
| Fluid Compressibility | 4.00E-07 | 4.00E-07 | 4.00E-07 | 4.00E-07 /kPa |
| Total Compressibility | 1.60E-06 | 1.65E-06 | 1.40E-06 | 1.60E-06 /kPa |
| Permeability | 10 | 10 | 10 | 1 mD |

Intertank Properties:

| Flow Area (m ²) | Tank #1 | Tank #2 | Tank #3 | Tank #4 (Aquifer) |
|-----------------------------|---------|---------|---------|-------------------|
| Tank #1 | - | - | - | - |
| Tank #2 | - | - | - | - |
| Tank #3 | - | - | - | - |
| Tank #4 | - | - | - | - |

| Distance (m) | Tank #1 | Tank #2 | Tank #3 | Tank #4 |
|--------------|---------|---------|---------|---------|
| Tank #1 | - | 800 | 800 | 800 |
| Tank #2 | 800 | - | 800 | 800 |
| Tank #3 | 800 | 800 | - | 800 |
| Tank #4 | 800 | 800 | 800 | - |

| Transmissibility (m ³ /d/kPa) | Tank #1 | Tank #2 | Tank #3 | Tank #4 |
|--|---------|---------|---------|---------|
| Tank #1 | - | - | - | - |
| Tank #2 | - | - | - | - |
| Tank #3 | - | - | - | - |
| Tank #4 | - | - | - | - |

Wellbore Properties:

| | |
|----------------|----------|
| Tubing ID | 0.219 m |
| Pipe Roughness | 0.046 mm |

| Transmissibility (m ³ /d/kPa) | Tank #1 | Tank #2 | Tank #3 |
|--|---------|---------|---------|
| J _w | 0.20 | 0.30 | 0.40 |

| | Tank #1 | Tank #2 | Tank #3 |
|------------|---------|---------|---------|
| Depth (m3) | 1,000 | 1,025 | 1,050 |

Control Conditions:

| | |
|----------------------------|------------------------|
| Minimum THP | 4000 kPa |
| Minimum Rate | 200 m ³ /d |
| Target Rate | 6000 m ³ /d |
| Max Time Step | 15 days |
| Max Pressure Drop per Step | 50 kPa |
| Minimum Time Step | 5 days |

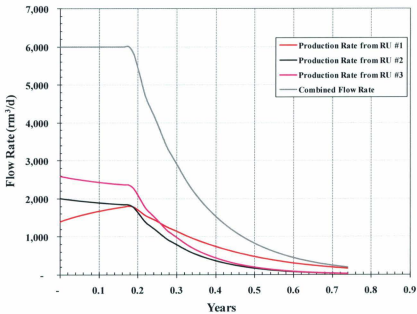


Figure 36: Wellbore Production for Three Non-Communicating Tanks without Aquifer Output

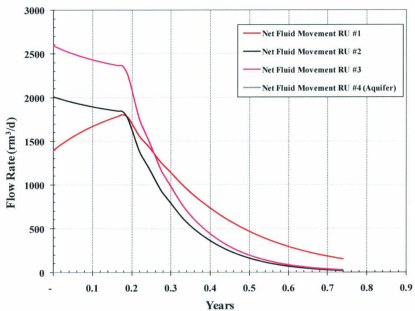


Figure 37: RU Production for Three Non-Communicating Tanks without Aquifer Output

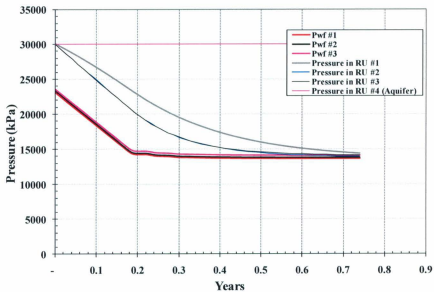


Figure 38: RU Pressure for Three Non-Communicating Tanks without Aquifer Output

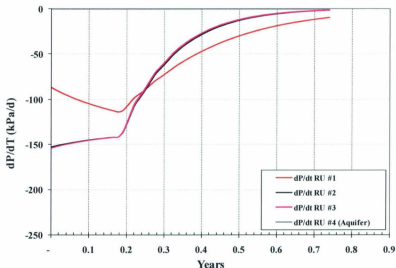


Figure 39: Pressure Depletion for Three Non-Communicating Tanks without Aquifer Output

4.5.1 Discussion of Results

This case demonstrates that the solving routine can solve for the depletion of multiple tanks. The results show the relative contribution from each tank is a function of the well transmissibility, the depth of the perforations, the compressibility and initial pore volume differences between the three reservoir units.

[Figure 36](#) demonstrates varying wellbore production rates over the life of the project, which is determined by reservoir pressure, wellbore transmissibility, and

downhole producing pressure. This provides the opportunity for interwell crossflow during any shut-in periods.

4.6 Three Partially-Communicating Tanks, With Partial Aquifer

This case represents a production well draining three reservoir units of which two are connected and partially supported by a common aquifer connected to two of the reservoir units.

The input assumptions are presented in Figure 40 [Error! Reference source not found.](#) with the output presented in [Figure 41](#) through [Figure 44](#).

Scenario Schematic:

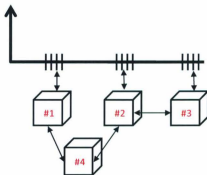


Figure 40: Three Partially-Communicating Tanks with Partial-Aquifer Input

Fluid Properties:

| | |
|-----------------------------|-----------------------------------|
| Viscosity | 0.5 mPas |
| Density | 980 kg/m ³ |
| Formation Volume Factor | 1 m ³ /sm ³ |
| Relative Phase Permeability | 0.7 Relative to Air |

Reservoir Unit Properties:

| | Tank #1 | Tank #2 | Tank #3 | Tank #4 (Aquifer) |
|--------------------------|------------|-----------|------------|---------------------------|
| Initial Pressure | 30,000 | 30,000 | 30,000 | 30,000 kPa |
| Initial Bulk Volume | 5.0E+07 | 4.0E+07 | 6.0E+07 | 1.5E+08 m ³ |
| Initial Fluid Saturation | 100% | 100% | 100% | 100% |
| Initial Porosity | 20% | 20% | 20% | 20% |
| Initial Pore Volume | 10,000,000 | 8,000,000 | 12,000,000 | 30,000,000 m ³ |
| Rock Compressibility | 1.20E-06 | 1.25E-06 | 1.00E-06 | 1.20E-06 /kPa |
| Fluid Compressibility | 4.00E-07 | 4.00E-07 | 4.00E-07 | 4.00E-07 /kPa |
| Total Compressibility | 1.60E-06 | 1.65E-06 | 1.40E-06 | 1.60E-06 /kPa |
| Permeability | 10 | 10 | 10 | 1 mD |

Intertank Properties:

| Flow Area (m ²) | Tank #1 | Tank #2 | Tank #3 | Tank #4 (Aquifer) |
|-----------------------------|---------|---------|---------|-------------------|
| Tank #1 | - | - | - | 800 |
| Tank #2 | - | - | 150 | 500 |
| Tank #3 | - | 150 | - | - |
| Tank #4 | - | 500 | - | - |

| Distance (m) | Tank #1 | Tank #2 | Tank #3 | Tank #4 |
|--------------|---------|---------|---------|---------|
| Tank #1 | - | 800 | 800 | 800 |
| Tank #2 | 800 | - | 800 | 800 |
| Tank #3 | 800 | 800 | - | 800 |
| Tank #4 | 800 | 800 | 800 | - |

| Transmissibility (m ² /d/kPa) | Tank #1 | Tank #2 | Tank #3 | Tank #4 |
|--|---------|---------|---------|---------|
| Tank #1 | - | - | - | 0.22 |
| Tank #2 | - | - | 0.23 | 0.14 |
| Tank #3 | - | 0.23 | - | - |
| Tank #4 | 0.22 | 0.14 | - | - |

Wellbore Properties:

| | |
|----------------|----------|
| Tubing ID | 0.219 m |
| Pipe Roughness | 0.046 mm |

| | | | |
|--|---------|---------|---------|
| Transmissibility ($\text{rm}^3/\text{d}/\text{kPa}$) | Tank #1 | Tank #2 | Tank #3 |
| Jw | 0.20 | 0.30 | 0.40 |

| | | | |
|------------|---------|---------|---------|
| | Tank #1 | Tank #2 | Tank #3 |
| Depth (m3) | 1,000 | 1,025 | 1,050 |

Control Conditions:

| | |
|----------------------------|----------------------------|
| Minimum THP | 4000 kPa |
| Minimum Rate | 200 m^3/d |
| Target Rate | 6000 m^3/d |
| Max Time Step | 15 days |
| Max Pressure Drop per Step | 50 kPa |
| Minimum Time Step | 5 days |

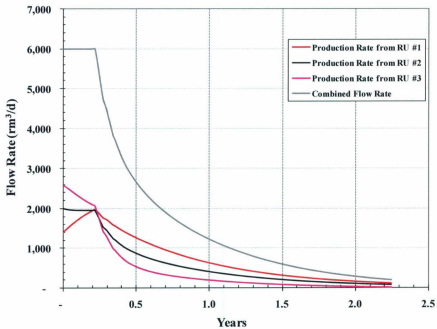


Figure 41: Wellbore Production for Three Partially-Communicating Tanks with Partial-Aquifer Output

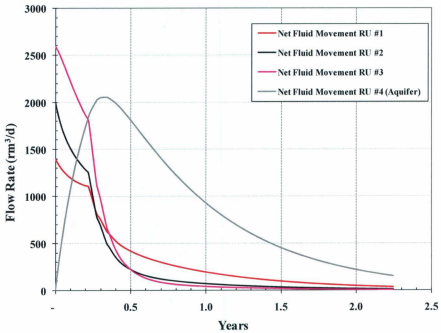


Figure 42: RU Production for Three Partially-Communicating Tanks with Partial-Aquifer Output

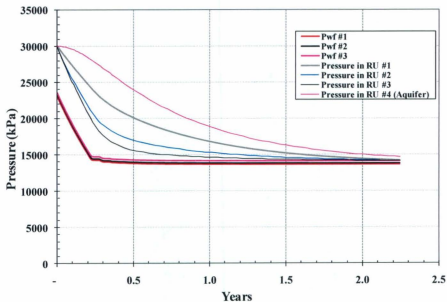


Figure 43: RU Pressure for Three Partially-Communicating Tanks with Partial-Aquifer Output

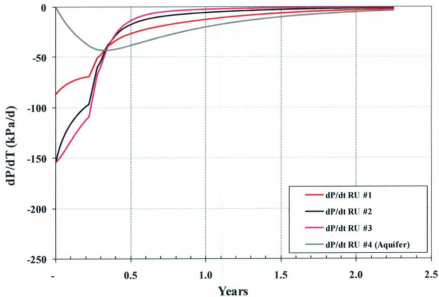


Figure 44: Pressure Depletion for Three Partially-Communicating Tanks with Partial-Aquifer Output

4.6.1 Discussion of Results

This case demonstrates that the solving routine can solve for the depletion of multiple tanks with varying degrees of communication. The results show the relative contribution from each tank is a function of the well transmissibility, the depth of the perforations, the compressibility and initial pore volume differences between the three reservoir units plus the intertank communication pathway.

One important observation from this scenario is the change in relative wellbore production from the connected RU and how it changes through time dependant of the transmissibilities and tank pressure, refer to [Figure 41](#)[Figure-41](#).

4.7 Comparison of Scenarios

[Figure 45](#)[Figure-45](#) shows the total production rate of the wellbore under the various scenarios presented. From this, some general observations can be made about both the physical situation being modeled as well as the modeling procedure.

The first observation relates to the general productivity. It is clear from [Figure 45](#)[Figure-45](#) that the greater the connection to the reservoir results in greater initial productivity as demonstrated by looking at the one tank, two tank, and three tank scenarios. In the one tank scenario, the 6000 m³/d production target cannot be achieved while the three tank scenario is able to achieve this target and sustain the rate for at least 3 months. When evaluating development scenarios, a petroleum engineer could utilize this model to evaluate the benefit of achieving an extended production profile versus the cost of drilling additional well length.

The second observation relates to the decline. [Figure 45](#)[Figure-45](#) again shows that scenarios with aquifers how a slower decline, and hence a greater ultimate recovery. A petroleum engineer would be able to perform pre-development sensitivity scenarios on aquifer size and strength and the resultant impact on the wells

productive life. Post-production, history matching would also be possible to better understand the size and transmissibility of the aquifer.

A third observation relates to the two tank scenarios where the transmissibility between the tanks does not impact the combined production rate, even though the relative contribution is substantially impacted, refer to [Figure 26](#) and [Figure 31](#). This is represented in reality in the situation where a horizontal production crosses a fault. From the total production from the well it is very unlikely that the transmissibility across that fault can be determined in the near wellbore region without additional downhole information such as pressure transient analysis and or production logging information.

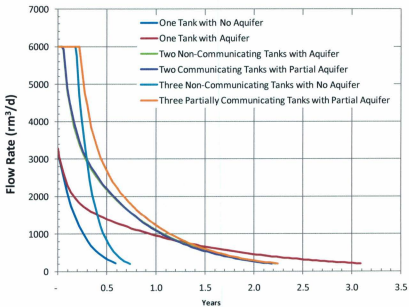


Figure 45: Total Production Rate Comparison

5.0 General Discussion of Results

Overall, the predicted model results agree with generally expected reservoir behavior, implying that the method described in this thesis has the ability to provide a usable platform for reservoir simulation. Potential uses of the method of simulation could include applications with faulted reservoirs with communicating or non-communicating faults, reservoirs with a connected aquifer, multiple reservoirs communicating through a common aquifer, a multi-layered reservoir of variable reservoir quality, a wellbore draining multiple reservoirs, or any system where an appreciable pressure gradient could exist.

This type of model can be used to quickly diagnose and history match production performance from new fields to identify reservoir properties involving effective reservoir volume, the presence of faults or baffles, the transmissibility and strength of connected aquifers.

Tanks modeling can also be used to quickly investigate pre-drill scenarios involving well length compared to well cost, sensitivities on deliverability for short and long-term depletion scenarios.

5.1 Novelty of Research

The genesis of this body work grew from the need for more efficient modeling of complex and compartmentalized reservoirs, as is typical in the highly faulted hydrocarbon producing basins of the coast of Newfoundland.

This is the first time the concept of multiple reservoir units and aquifers treated as individual tanks were solved as a system of ordinary differential equations, to the authors knowledge.

Furthermore, this work also discussed the future potential for combining this tank modeling concept with an advanced well hydraulics models with connectivity wells for enhancing reservoir unit communication.

Finally, this work discussed how these novel methods can be improved to increase accuracy and applicability without sacrificing the CPU advantages these methods have over the use of conventional reservoir simulators.

5.2 Limitations

There are several limitations in this work, however all of these can be overcome with additional study and implementation. These limitations stem from the assumptions used to simplify the modeling process at this stage in the work, to allow for focus on the multiple reservoir units integration.

One of the fundamental and limiting assumptions is the assumption of single phase constant compressibility. Moving past these simplifications could be relatively easy. This includes the inclusion of a black-oil material balance model as described by R. J. Schilthuis (Schilthuis, 1935). In this widely used black-oil model, the components of the reservoir system (rock, oil, water, gas) and their compressibility and net cumulative withdrawals can be used to predict pressure, or if pressure is known, a prediction of the original fluid volumes is possible. In this model, single phase behavior is not assumed which has proven to be a very powerful and popular reservoir engineering tool. Schilthuis' model is often shown in the form in Equation 5-1.

$$N = \frac{N_p [B_o + (R_p - R_g) B_g] - (W_e - W_p + W_i) B_w - G_i B_g}{(B_o - B_{oi}) + (R_{oi} - R_g) B_g + m B_{wi} \left(\frac{B_g - B_{Ri}}{B_{gi}} \right) + \left(\frac{B_{wi}}{1 - S_{wi}} \right) (1 + m) (S_{wi} c_w + c_r) (P_{Ri} - P_R)}$$

(5-1)

where:

B_g = Gas formation volume factor at current pressure, m^3/m^3

B_o = Oil formation volume factor at current pressure, m^3/m^3

B_{oi} = Original oil formation volume factor, m^3/m^3

B_w = Water formation volume factor at current pressure, m^3/m^3

c_w = water compressibility at current pressure, kPa^{-1}

c_r = rock compressibility at current pressure, kPa^{-1}

G_i = Original gas in place, sm^3

N_p = Cumulative oil production, sm^3

N = Original oil in place, sm^3

m = ratio of original gas in place to original oil in place

P_{Ri} = Initial reservoir pressure, kPa

P_R = Current reservoir pressure, kPa

R_p = Produced gas oil ratio, m^3/m^3

R_s = Solution gas oil ratio at current pressure, m^3/m^3

R_{si} = Original solution gas oil ratio, m^3/m^3

S_{wi} = Water saturation as a fraction of the effective pore space

W_e = Cumulative water influx, sm^3

W_i = Cumulative water injected, sm^3

W_p = Cumulative water production, sm^3

Another limitation is single-phase flow, both in the wellbore model and in the reservoir units. The concepts of relative permeability and the resultant fractional flow could be implemented for the reservoir units. This will allow for different tanks to have different fluid fractions as well as for different portion of the wellbore to have difference fluid production splits (i.e. watercut or gas-oil-ratio). This would then extend to allow for multi-phase flow correlations to be used for the wellbore modeling. For example, the Hagedorn and Brown method (Hagedorn and Brown,

1965) could be implemented for vertical flow while the Beggs and Brill method could be implemented for slightly inclined and horizontal wells (Beggs and Brill, 1973) or any other method desired.

6.0 Conclusions

The question that we were investigating was: Can conventional material balance calculations be used to provide realistic long-term depletion forecasts in an efficient method that solves complex, multi-tank communicating, reservoir systems? Can these systems be integrated with advanced wellbore modeling techniques to increase the reliability of our predictions?

This work successfully demonstrated the integration of aquifers models, tank reservoirs, inter-tank transmissibility, well transmissibility, and wellbore performance into an integrated model that was used to predict future well performance. The underlying themes were that a characteristic relationship between flow rate and pressure difference is linked by transmissibility and that there is a relationship between total compressibility and pressure in combination with the fact the reservoirs and wellbores can be modeled with the same thematic relationships. Where the following equations apply

$$q = \frac{dV}{dt} = J(P_1 - P_2) \quad (6-1)$$

$$c_i = -\frac{1}{V_i} \frac{dV}{dP} \quad (6-2)$$

This work demonstrated the successful integration of aquifers, reservoir tanks, well inflow, and wellbore modeling into an integrated system that can quickly be used as a tool for investigating the petroleum systems. Scenarios involving a single reservoir tank, multiple communicating reservoir tanks, multiple tanks with variable communication to supporting aquifers, and wellbores with multiple inflow regions were all successfully demonstrated.

This work is directly applicable to many real-world reservoirs including faulted reservoirs with communicating or non-communicating faults, reservoirs with a connected aquifer, multiple reservoirs communicating through a common aquifer, a multi-layered reservoir of variable reservoir quality, a wellbore draining multiple reservoirs, or any system where an appreciable pressure gradient could exist

This work can form a fundamental module enabling the calculation of coupled wellbore and reservoir models with advanced completion technologies.

7.0 Recommendations

Once the limitations of single-phase flow and constant compressibility are overcome, more complex flow could be incorporated within the reservoir unit concept. This could include one-dimensional displacement calculations as well as the implementation of water/oil or gas/oil coning within the reservoir units, such as the work completed by Chaperon (Chaperon, 1986).

The well inflow model could be expanded to include time-dependent transmissibility, such as during different flow conditions or deteriorating productivity. The inflow model can also be expanded to include typical industry models such as Babu & Odeh, Joshi, or others.

A simplistic approach was made to wellbore modeling in this work to prove the concept, but is not suitable for a wide range of typical oilfield operating conditions. Future investigations should include multiphase flow where more than one phase is present and the phase fraction changes as a function of pressure and temperature. This way the applicability could be encompassed to include both oil and gas wells under a variety of fluid states and conditions. This could involve future investigations into multiphase pressure drop correlations, such as those by Hagendorf and Brown, Beggs and Brill, and others. In addition, this would be a valuable addition when coupled with a multiphase reservoir or black oil modeling techniques were investigated.

References

- 1 Ahmed, T., "Reservoir Engineering Handbook Third Edition" Oxford, UK: Elsevier Inc., 2006.
- 2 Atkinson, K., Han, W., "Elementary Numerical Analysis", John Wiley & Son, Inc. 2004.
- 3 Autar, K., University of South Florida,, "Ordinary Differential Equations", Textbook notes, 2009.
- 4 Babu, D.K., Odeh, A.S.. "Productivity of a Horizontal Well", SPERE, Page 417, November 1989.
- 5 Beggs, D.H., Brill, J.P., AIME U. of Tulsa, "A Study of Two-Phase Flow in Inclined Pipes", SPE #4007, Presented at SPE-AIME 47th Annual Fall Meeting, San Antonio Tex., October 8-11, 1972.
- 6 Benedict, Robert P., "Fundaments of Pipe Flow". New York: John Wiley & Sons Inc., 1980.
- 7 Billo, E. Joseph. "Excel for Scientists and Engineers: Numerical Methods", Hoboken New Jersey: John Wiley & Sons, Inc., 2007.
- 8 Blasius, P.R.H., "Das Aehnlichkeitsgesetz bei Reibungsvorgangen in Flussigkeiten", Phys. Z. Vol. 12, 1911, p. 1175, 1911. Translated as "The law of similarity applied to frictional phenomena".
- 9 Butcher, J.C., University of Auckland, G. Wanner, University of Geneva, "Runge-Kutta Methods: Some Historical Notes." Applied Numerical Mathematics 22 (1996) 113-151, 1996.
- 10 Carter R.D. AIME, Tracy G.W. AIME, Pan American Petroleum Corp., . "An Improved Method for Calculating Water Influx", SPE 1626-G. Original manuscript received August 30 1960. Revised manuscript received November 3 1960.
- 11 Chaperon, I. Total-CFP. "Theoretical Study of Coning Toward Horizontal and Vertical Wells in Anisotropic Formation: Subcritical and Critical Rates". SPE 15377, Presented at the 61st Annual Technical Conference and

- Exhibition of the Society of Petroleum Engineers held in New Orleans, LA
October 5-8, 1986.
- 12 Colebrook, C. F., "*Turbulent Flow in Pipes, with Particular Reference to the Transition Region Between the Smooth and Rough Pipe Laws*", J. Inst. Civil Eng., London, Vol. 11, p. 133, 1938-1939.
 - 13 Chen, N.H., "*An Explicit Equation for Friction Factor in Pipe. Industrial Engineering Chemical Fundamentals*", 18 (2), pp 296-297. 1979.
 - 14 Dake, L.P., "*Fundamentals of Reservoir Engineering*", Amsterdam, The Netherlands, Elsevier Inc., 1978.
 - 15 Darcy, H.P.G. "*Experimental Research on the Flow of Water in Pipes (in French)*", Mem. Acad. Sci.Inst. Imp. Fr., Vol. 15., p.141, 1858.
 - 16 Fanchi, J.R. "*Principles of Applied Reservoir Simulation Third Edition*". Oxford, UK: Elsevier Inc., 2006.
 - 17 Fetkovich, M.J., SPE-AIME, Phillips Petroleum Co., "*A Simplified Approach to Water Influx Calculations – Finite Aquifer Systems*", SPE 2603. Revised manuscript received April 8, 1971. Presented at SPE 44th Annual Fall Meeting, Denver Colorado September 28 – October 1 1969.
 - 18 Furui, K., Zhu, D., Hill, A.D., The University of Texas at Austin, "*A Rigorous Formation Damage Skin Factor and Reservoir Inflow Model for a Horizontal Well*", SPE 74698. Presented at the SPE International Symposium and Exhibition on Formation Damage Control held in Louisiana 20-21 February 2002.
 - 19 Guo, B., Lyons, W.C., Ghalambor, A., "*Petroleum Production Engineering A Computer-Assisted Approach*", Oxford, UK: Elsevier Science and Technology Books, 2007.
 - 20 Haaland, SE. "*Simple and Explicit Formulas for the Friction Factor in Turbulent Flow*", Journal of Fluids Engineering (ASME) volume 103, pages 89–90. 1983.
 - 21 Halliburton, Landmark Software and Services. "*NETool A Near-Wellbore and Completion Hydraulics Simulator*", www.Halliburton.com, May 2010.

- 22 Hagedorn, A.R., Brown, K.E., "Experimental Study of Pressure Gradients Occurring During Continuous Two-Phase Flow in Small-Diameter Conduits", J. Petroleum Technology, p. 475, 1965.
- 23 Havlena, D. and Odeh, A.S., "The Material Balance as an Equation of a Straight Line", J.Pet.Tech. August: 896-900. Trans., AIME, 228, 1963.
- 24 Havlena, D. and Odeh, A.S., "The Material Balance as an Equation of a Straight Line. Part II - Field Cases", J.Pet.Tech. July: 815-822. Trans., AIME., 231, 1964.
- 25 Hurst, W. AIME, Petroleum Consultant, "The Simplification of the Material Balance Formulas by the Laplace Transformation", SPE 1030-G. Original manuscript received February 5 1958, revised manuscript received July 1 1958. Presented at Production and Reservoir Engineering Conference in Tulsa, Oklahoma, March 20-21, 1958.
- 26 Joshi, S.D.. "Augmentation of Well Productivity with Slant and Horizontal Wells", Journal of Petroleum Technology. June 1998 pages 729 – 739.
- 27 Khoriakov, V, Johansen, A.C., Johansen, T. E.. "Transient Flow Modeling of Advanced Wells (Draft)", Memorial University of Newfoundland, Canada, 2010.
- 28 Marques, J.B., SPE, Petrobras S.A., Trevisan, O.V., SPE, and Suslick S.B., SPE, Unicamp.. "Classic Models of Calculation of Influx: A Comparative Study", SPE 107265. Presented at the 2007 SPE Latin American and Caribbean Petroleum Engineering Conference, Buenos Aires, Argentina, 15-18 April 2007.
- 29 Moody, L., "Friction Factors for Pipe Flow", ASME Transactions Volume 66, Page 671, 1944.
- 30 Nikaradse, J., "Laws of Flow in Rough Pipes", Forsch.-Arb. Ing.-Wesen, No. 361, 1933.
- 31 Odeh, A.S., Jones, I.G., Socony Mobil Oil Co., Inc., "Pressure Drawdown Analysis, Variable-Rate Case", SPE 1084. Presented at SPE Production Research Symposium held in Tulsa Okla. May 3-4, 1965.

- 32 Peaceman, D.W., SPE, Consultant/Western Atlas Software. "*Representation of a Horizontal Well in Numerical Reservoir Simulation*", SPE 21217. SPE Advanced Technology Series, Vol. 1, No. 1, 1993.
- 33 Peaceman, D.W., SPE, Consultant/Western Atlas Software. "*A New Method for Representing Multiple Wells with Arbitrary Rates in Numerical Reservoir Simulation*", SPE 29120. SPE Reservoir Engineering, November 1995.
- 34 Penmatcha, V.R., Aziz, K. 1999. "*Comprehensive Reservoir/Wellbore Model for Horizontal Wells*", SPE Journal, Vol. 4, No. 3, September 1999.
- 35 Petroleum Experts Ltd., "*MBAL Online Help Manual*", Petroleum Experts Ltd., March 2009.
- 36 Prandtl, L. "*Neuere ergebnisse der turbulenzforschung*", Z. VDI, Vol. 77, p. 105, 1933.
- 37 Schilthuis, R.J., "*Active Oil and Reservoir Energy*", Trans., AIME, 118: 33-52, 1936.
- 38 Standing, M.B., "*Concerning the calculation of inflow performance of wells producing from solution gas drive reservoirs*", Journal of Petroleum Technology, pages 1141-1142, September 1971.
- 39 T.E. Johansen, "*Advanced Well Completion and Optimization*", Joint Industry Project Presentation, Denver, 2008.
- 40 Uren, L.C., "*Petroleum Production Engineering, Oil Field Exploitation 3rd Edition*", McGraw-Hill Book Company Inc., New York, 1953.
- 41 Van Everdingen, A.F., Shell Oil Co., Houston, and Hurst, W., Petroleum Consultant, Houston, Members AIME, "*The Application of the Laplace Transformation to Flow Problems in Reservoirs*", SPE 949305, Paper presented at the AIME Annual Meeting in San Francisco, February 13-17, 1949.
- 42 Vogel, J.V., "*Inflow Performance Relationships for Solution Gas Drive Wells*", Journal of Petroleum Technology, pages 83 - 92, January 1968.

- 43 Vogt, J.P., Wang, B. Texaco USE. "*Accurate Formulas for Calculating the Water Influx Superposition Integral*", SPE 17066, Presented at the SPE Eastern Regional Meeting held in Pittsburgh, Pennsylvania, October 21-23, 1987.
- 44 Watts, J.W., Reservoir Simulation: "*Past, Present, and Future. SPE Computer Applications*", December 1997.
- 45 Weisbach, J.. "*Mechanics of Engineering*", Van Nostrand, 1872.

Appendix

A. Numerical Method Approach

The system of units creates a system of ordinary differential equations (ODEs) of the initial boundary type. That is, the initial volume and pressure is known at each time step.

As the number of reservoir units increases, the system of ODEs increases as well, dictated by the number of reservoir units and the number of connections between tanks. This makes the representation of these systems into a closed form impossible, and it becomes convenient to seek an approximate solution by means of numerical methods.

The reservoir units form a series of first-order differential equations of the form:

$$\frac{dy_i}{dx} = f(x, y_1, y_2, \dots, y_N) \quad (1)$$

For the real-valued function of y of the real variable x , where $y' \equiv dy/dx$ and f is a given real-valued function of two real variables.

The differential equation will be considered in tandem with an initial condition so, that given two real numbers x_0 and y_0 , we can seek a solution for $x > x_0$ such that

$$y(x_0) = y_0 \quad (2)$$

These two equations together represent an initial value problem.

The 4th Order Runge-Kutta (RK) Method was chosen to solve the series of ordinary differential equations generated by the system of units being evaluated in the modeling. The 4th Order is the most common of the RK methods because of the ease of use and high numerical order. This method also provide a high degree of accuracy in an efficient manner.

The RK method for solving a system of ordinary differential equations works under the following principle.

$$y_{i+1} = y_i + (a_1k_1 + a_2k_2 + a_3k_3 + a_4k_4)h \quad (3)$$

If we know the value of $y = y_i$ at x_i , we can find the value of $y = y_{i+1}$ at x_{i+1} , and $h = x_{i+1} - x_i$.

Equation 88 can be equated to the first five terms of the Taylor series expansion.

$$y_{i+1} = y_i + \frac{dy}{dx} \Big|_{x_i, y_i} (x_{i+1} - x_i) + \frac{1}{2!} \frac{d^2y}{dx^2} \Big|_{x_i, y_i} (x_{i+1} - x_i)^2 + \frac{1}{3!} \frac{d^3y}{dx^3} \Big|_{x_i, y_i} (x_{i+1} - x_i)^3 + \frac{1}{4!} \frac{d^4y}{dx^4} \Big|_{x_i, y_i} (x_{i+1} - x_i)^4 \quad (4)$$

Knowing that

$$\frac{dy}{dx} = f(x, y)$$

and

$$x_{i+1} - x_i = h$$

we get

$$y_{i+1} = y_i + f(x_i, y_i)h + \frac{1}{2!} f'(x_i, y_i)h^2 + \frac{1}{3!} f''(x_i, y_i)h^3 + \frac{1}{4!} f'''(x_i, y_i)h^4 \quad (5)$$

Based on equating Equation 4 and Equation 5, one of the more popular solutions used is

$$y_{i+1} = y_i + \frac{1}{6}(k_1 + 2k_2 + 2k_3 + k_4)h \quad (6)$$

With

$$k_1 = f(x_i, y_i)h \quad (7)$$

$$k_2 = f(x_i + \frac{1}{2}h, y_i + \frac{1}{2}k_1h) \quad (8)$$

$$k_3 = f(x_i + \frac{1}{2}h, y_i + \frac{1}{2}k_2h) \quad (9)$$

$$k_4 = f(x_i + h, y_i + k_3h) \quad (10)$$

Sometimes a system is described by several differential equations, as is the case in Section 3.03-0. The Runge-Kutta formulas can be used to solve systems of simultaneous differential equations.

For a system with independent variable x , N dependant variables y_i and N differential equations

$$\frac{dy_i}{dx} = f(x, y_1, y_2, \dots, y_N) \quad (11)$$

the relationships are:

$$k_{1i} = f_i(x, y_1, y_2, \dots, y_N)h \quad (12)$$

$$k_{2i} = f_i(x_1 + \frac{1}{2}h, y_1 + \frac{1}{2}k_{11}h, y_2 + \frac{1}{2}k_{12}h, \dots, y_N + \frac{1}{2}k_{1N}h) \quad (13)$$

$$k_{3i} = f_i(x_1 + \frac{1}{2}h, y_1 + \frac{1}{2}k_{21}h, y_2 + \frac{1}{2}k_{22}h, \dots, y_N + \frac{1}{2}k_{2N}h) \quad (14)$$

$$k_{4i} = f_i(x_1 + h, y_1 + k_{31}h, y_2 + k_{32}h, \dots, y_N + k_{3N}h) \quad (15)$$

and

$$y_{i+1} = y_i + \frac{1}{6}(k_{1i} + 2k_{2i} + 2k_{3i} + k_{4i}) \quad (16)$$

In our case, x denotes time and y denotes pressure in each reservoir unit. Hence, with N reservoir units, there will be N systems of equations that require solving for each time x .

B. Excel Main Calculation Sheet (Part A)

| t (d) | dPA1/dt (kPa/d) | dPr1/dt (kPa/d) | dPr2/dt (kPa/d) | dPr3/dt (kPa/d) | dWw/dt (kPa/d) | dvr1/dt | dvr2dt | dvr3/dt | Pa1 (kPa) | Pr1 (kPa) | Pr2 (kPa) | Pr3 (kPa) | CumWw1 (m3) | CumVr1 (m3) | CumVr2 (m3) |
|----------|--------------------|--------------------|--------------------|--------------------|-------------------|---------|--------|---------|--------------|--------------|--------------|--------------|----------------|----------------|----------------|
| 0 | 0 | -52 | -89 | - | - | 829 | 1,171 | - | 30,000 | 30,000 | 30,000 | 30,000 | - | - | - |
| 10 | 0 | -54 | -86 | - | - | 866 | 1,134 | - | 30,000 | 29,513 | 29,206 | 30,000 | - | 7,791 | 10,476 |
| 20 | 0 | -56 | -84 | - | - | 897 | 1,103 | - | 30,000 | 29,004 | 28,438 | 30,000 | - | 15,939 | 20,622 |
| 30 | 0 | -58 | -82 | - | - | 923 | 1,077 | - | 30,000 | 28,477 | 27,689 | 30,000 | - | 24,360 | 30,487 |
| 40 | 0 | -59 | -80 | - | - | 946 | 1,054 | - | 30,000 | 27,934 | 26,958 | 30,000 | - | 33,040 | 40,114 |
| 50 | 0 | -61 | -79 | - | - | 965 | 1,035 | - | 30,000 | 27,377 | 26,241 | 30,000 | - | 41,931 | 49,539 |
| 60 | 0 | -62 | -78 | - | - | 981 | 1,019 | - | 30,000 | 26,808 | 25,537 | 30,000 | - | 51,001 | 58,790 |
| 70 | 0 | -63 | -77 | - | - | 995 | 1,005 | - | 30,000 | 26,229 | 24,843 | 30,000 | - | 60,224 | 67,895 |
| 80 | 0 | -63 | -76 | - | - | 1,007 | 993 | - | 30,000 | 25,642 | 24,158 | 30,000 | - | 69,577 | 76,875 |
| 90 | 0 | -64 | -75 | - | - | 1,017 | 983 | - | 30,000 | 25,047 | 23,480 | 30,000 | - | 79,039 | 85,750 |
| 100 | 0 | -65 | -74 | - | - | 1,025 | 975 | - | 30,000 | 24,445 | 22,808 | 30,000 | - | 88,594 | 94,534 |
| 110 | 0 | -65 | -74 | - | - | 1,033 | 967 | - | 30,000 | 23,838 | 22,141 | 30,000 | - | 98,228 | 103,241 |
| 120 | 0 | -66 | -74 | - | - | 1,039 | 961 | - | 30,000 | 23,226 | 21,478 | 30,000 | - | 107,939 | 111,883 |
| 130 | 0 | -66 | -73 | - | - | 1,044 | 956 | - | 30,000 | 22,611 | 20,819 | 30,000 | - | 117,687 | 120,470 |
| 140 | 0 | -66 | -73 | - | - | 1,048 | 952 | - | 30,000 | 21,991 | 20,163 | 30,000 | - | 127,493 | 129,009 |
| 150 | 0 | -67 | -73 | - | - | 1,052 | 948 | - | 30,000 | 21,368 | 19,510 | 30,000 | - | 137,339 | 137,509 |
| 160 | 0 | -67 | -73 | - | - | 1,055 | 945 | - | 30,000 | 20,743 | 18,858 | 30,000 | - | 147,220 | 145,974 |
| 170 | 0 | -67 | -73 | - | - | 1,058 | 942 | - | 30,000 | 20,115 | 18,207 | 30,000 | - | 157,130 | 154,409 |
| 180 | 0 | -67 | -73 | - | - | 1,060 | 940 | - | 30,000 | 19,485 | 17,558 | 30,000 | - | 167,064 | 162,820 |
| 190 | 0 | -66 | -69 | - | - | 1,034 | 896 | - | 30,000 | 18,853 | 16,910 | 30,000 | - | 177,019 | 171,210 |
| 215 | 0 | -48 | -39 | - | - | 753 | 503 | - | 30,000 | 17,445 | 15,597 | 30,000 | - | 195,162 | 188,191 |
| 240 | 0 | -35 | -22 | - | - | 552 | 289 | - | 30,000 | 16,419 | 14,860 | 30,000 | - | 215,285 | 197,718 |
| 265 | 0 | -26 | -13 | - | - | 407 | 169 | - | 30,000 | 15,665 | 14,436 | 30,000 | - | 237,108 | 203,180 |
| 280 | 0 | -19 | -8 | - | - | 297 | 97 | - | 30,000 | 15,110 | 14,188 | 30,000 | - | 255,807 | 206,376 |
| 315 | 0 | -14 | -4 | - | - | 217 | 56 | - | 30,000 | 14,703 | 14,044 | 30,000 | - | 242,171 | 208,220 |

Excel Main Calculation Sheet (Part B)

| t (d) | dVw1/dt | dVw2/dt | dVw3/dt | Pbh1 (kPa) | Pbh2 (kPa) | Pbh3 (kPa) | Pthp (kPa) | dVwt/dt | Wa1 (rm3) | Vr1 (rm3) | Vr2 (rm3) | Vr3 (rm3) |
|----------|---------|---------|---------|---------------|---------------|---------------|---------------|---------|--------------|--------------|--------------|--------------|
| 0 | 829 | 1,171 | - | 25,856 | 26,096 | 26,336 | 16,242 | 2,000 | 30,000,000 | 10,000,000 | 8,000,000 | 12,000,000 |
| 10 | 866 | 1,134 | - | 25,184 | 25,425 | 25,666 | 15,502 | 2,000 | 30,000,000 | 9,992,209 | 7,989,524 | 12,000,000 |
| 20 | 897 | 1,103 | - | 24,520 | 24,761 | 25,001 | 14,837 | 2,000 | 30,000,000 | 9,984,071 | 7,979,378 | 12,000,000 |
| 30 | 923 | 1,077 | - | 23,860 | 24,101 | 24,341 | 14,178 | 2,000 | 30,000,000 | 9,975,640 | 7,969,513 | 12,000,000 |
| 40 | 946 | 1,054 | - | 23,204 | 23,445 | 23,685 | 13,521 | 2,000 | 30,000,000 | 9,966,960 | 7,959,886 | 12,000,000 |
| 50 | 965 | 1,035 | - | 22,551 | 22,792 | 23,032 | 12,869 | 2,000 | 30,000,000 | 9,958,069 | 7,950,461 | 12,000,000 |
| 60 | 981 | 1,019 | - | 21,901 | 22,142 | 22,382 | 12,219 | 2,000 | 30,000,000 | 9,948,999 | 7,941,210 | 12,000,000 |
| 70 | 995 | 1,005 | - | 21,253 | 21,494 | 21,734 | 11,571 | 2,000 | 30,000,000 | 9,939,776 | 7,932,105 | 12,000,000 |
| 80 | 1,007 | 993 | - | 20,607 | 20,848 | 21,088 | 10,924 | 2,000 | 30,000,000 | 9,930,423 | 7,923,125 | 12,000,000 |
| 90 | 1,017 | 983 | - | 19,962 | 20,203 | 20,443 | 10,280 | 2,000 | 30,000,000 | 9,920,961 | 7,914,250 | 12,000,000 |
| 100 | 1,025 | 975 | - | 19,318 | 19,559 | 19,799 | 9,636 | 2,000 | 30,000,000 | 9,911,406 | 7,905,466 | 12,000,000 |
| 110 | 1,033 | 967 | - | 18,675 | 18,916 | 19,156 | 8,993 | 2,000 | 30,000,000 | 9,901,772 | 7,896,759 | 12,000,000 |
| 120 | 1,039 | 961 | - | 18,033 | 18,274 | 18,514 | 8,351 | 2,000 | 30,000,000 | 9,892,071 | 7,888,117 | 12,000,000 |
| 130 | 1,044 | 956 | - | 17,391 | 17,632 | 17,872 | 7,709 | 2,000 | 30,000,000 | 9,882,313 | 7,879,530 | 12,000,000 |
| 140 | 1,048 | 952 | - | 16,750 | 16,991 | 17,231 | 7,068 | 2,000 | 30,000,000 | 9,872,507 | 7,870,991 | 12,000,000 |
| 150 | 1,052 | 948 | - | 16,109 | 16,349 | 16,590 | 6,426 | 2,000 | 30,000,000 | 9,862,661 | 7,862,491 | 12,000,000 |
| 160 | 1,055 | 945 | - | 15,467 | 15,708 | 15,948 | 5,785 | 2,000 | 30,000,000 | 9,852,780 | 7,854,026 | 12,000,000 |
| 170 | 1,058 | 942 | - | 14,826 | 15,067 | 15,307 | 5,144 | 2,000 | 30,000,000 | 9,842,870 | 7,845,591 | 12,000,000 |
| 180 | 1,060 | 940 | - | 14,184 | 14,425 | 14,666 | 4,502 | 2,000 | 30,000,000 | 9,832,936 | 7,837,180 | 12,000,000 |
| 190 | 1,034 | 896 | - | 13,682 | 13,923 | 14,163 | 4,000 | 1,930 | 30,000,000 | 9,822,981 | 7,828,790 | 12,000,000 |
| 215 | 753 | 503 | - | 13,680 | 13,921 | 14,161 | 4,000 | 1,256 | 30,000,000 | 9,800,838 | 7,811,809 | 12,000,000 |
| 240 | 552 | 289 | - | 13,657 | 13,898 | 14,138 | 4,000 | 841 | 30,000,000 | 9,784,715 | 7,802,282 | 12,000,000 |
| 265 | 407 | 169 | - | 13,633 | 13,873 | 14,113 | 4,000 | 575 | 30,000,000 | 9,772,892 | 7,796,820 | 12,000,000 |
| 290 | 297 | 97 | - | 13,622 | 13,863 | 14,103 | 4,000 | 395 | 30,000,000 | 9,764,193 | 7,793,624 | 12,000,000 |
| 315 | 217 | 56 | - | 13,618 | 13,858 | 14,099 | 4,000 | 273 | 30,000,000 | 9,757,829 | 7,791,780 | 12,000,000 |

C. Flowing Wellbore and Reservoir Solver

Sub SolveFlowing()

'Solver for Flowing Wellbore and Reservoir System

'Brandon Thomas

'Memorial University of Newfoundland

TARGET = Sheets("Main").Range("AB7").Value

MinTHP = Sheets("Main").Range("AB5").Value

MAXDP = Sheets("Main").Range("AB9").Value

MaxTS = Sheets("Main").Range("AB8").Value

MinTS = Sheets("Main").Range("AB10").Value

MINRATE = Sheets("Main").Range("AB6").Value

Sheets("MAIN").Select

Range("K23:AP1820").Select

Selection.ClearContents

Range("AI20").Select

ActiveCell.GoalSeek Goal:=TARGET, ChangingCell:=ActiveCell.Offset(0, -1)

ActiveCell.Offset(0, -23).Range("A1:AN1").Select

Selection.Copy

ActiveCell.Offset(0, 0).Range("A1").Select

ActiveSheet.Paste

ActiveCell.Offset(0, 23).Select

Range("AI21").Select

ActiveCell.GoalSeek Goal:=TARGET, ChangingCell:=ActiveCell.Offset(0, -1)

Do

Cut = 1

ActiveCell.Offset(0, -1).Value = ActiveCell.Offset(-1, -1).Value 'Shift to active line

Do

If MaxTS / Cut > MinTS Then ActiveCell.Offset(0, -24).Value = ActiveCell.Offset(-1, -24).Value + MaxTS / Cut

If MaxTS / Cut <= MinTS Then ActiveCell.Offset(0, -24).Value = ActiveCell.Offset(-1, -24).Value + MinTS

ActiveCell.GoalSeek Goal:=TARGET, ChangingCell:=ActiveCell.Offset(0, -1) 'Goal seek to match THP

THP = ActiveCell.Offset(0, -1).Value

If THP < MinTHP Then

ActiveCell.Offset(0, -1).Value = MinTHP 'Do not violate min THP

End If

ActiveCell.Offset(0, -23).Range("A1:AN1").Select 'Select Current Row

Selection.Copy 'Copy current row

ActiveCell.Offset(0, 0).Range("A1").Select 'Select current row

ActiveSheet.Paste 'Paste to current row to ensure RUNGE calculates fully

ActiveCell.Offset(0, 23).Select 'Select active cell

DP = Abs((ActiveCell.Offset(-1, -4).Value + ActiveCell.Offset(-1, -3).Value + ActiveCell.Offset(-1, -2).Value) / 3 - (ActiveCell.Offset(0, -4).Value + ActiveCell.Offset(0, -3).Value + ActiveCell.Offset(0, -2).Value) / 3)

Convergence = ActiveCell.Value - ActiveCell.Offset(-1, 0).Value

If ActiveCell.Offset(0, -24).Value - ActiveCell.Offset(-1, -24).Value = MinTS Then Exit Do

Cut = Cut * 2

Loop Until DP < MAXDP And Convergence <= 0

ActiveCell.Offset(1, -24).Value = ActiveCell.Offset(0, -24) + MaxTS

If ActiveCell.Offset(0, -1).Value < MinTHP Then ActiveCell.Offset(0, -1).Value = MinTHP 'Do not violate min THP

If ActiveCell.Offset(0, 0).Value < MINRATE Then Exit Do 'If flow rate lower than minimum finish calculation

ActiveCell.Offset(1, -23).Range("A1:AN1").Select 'Select next row

Selection.Copy 'Copy next row

ActiveCell.Offset(1, 0).Range("A1").Select 'Select target row

ActiveSheet.Paste 'Copy to target row

ActiveCell.Offset(-2, 23).Range("A1").Select 'Select active cell

ActiveCell.Offset(1, 0).Select 'Select next target cell

Counter = Counter + 1 'Progress counter

If Counter > 2000 Then Exit Do 'Limit total calculations to N+1

Loop

If Counter > 5 Then 'Do not delete first rows to maintain formulas in sheet

ActiveCell.Offset(0, -23).Range("A1:AM3").Select

Selection.ClearContents

End If

End Sub

'Single Phase Pressure Drop Calculation

'Brandon Thomas

'Memorial University of Newfoundland

Function UpstreamPressure(Dens, Visc, ID, Hup, Hdown, Lup, Ldown, E,
Pds, Rate) As Single

Dim Velocity As Single

Dim dL As Single

Dim dz As Single

Dim Re As Single

Dim f As Single

'Rate = Flow rate, m³/d [dV/dt]

'P in kPa

'Elevation change, m

dz = Hup - Hdown

'Length, m

dL = Lup - Ldown

'Flow velocity, m/s

$$\text{Rate} = \text{Rate} / 24 / 60 / 60$$

$$\text{Velocity} = \text{Abs}(\text{Rate} / 0.25 / 3.141592 / \text{ID}^2)$$

'Reynolds Number, Re

$$\text{Re} = \text{ID} * \text{Velocity} * \text{Dens} / (\text{Visc} / 1000)$$

'Fanning Friction Factor, f

$$\text{If Rate} > 0 \text{ Then } f = (1 / (-4 * \text{Log10}((E / 3.7065) - (5.0452 / \text{Re})) * \text{Log10}((E^2 / 1.1098 / 2.8257) + (7.149 / \text{Re})^{0.8981}))))^2$$

'Gravity Pressure Drop

$$dPg = (9.81 / 1) * \text{Dens} * dz / 1000$$

'Kinetic Pressure Drop

$$dPk = 0$$

'Friction Pressure Drop

$$dPf = 2 * f * \text{Dens} * \text{Velocity}^2 * dL / (1 * \text{ID}) / 1000$$

$$dPt = Pds + dPg + dPk + dPf$$

UpstreamPressure = dPt

End Function



